TWO NOVEL TRANSPORTERS ESSENTIAL FOR REASSIMILATION OF CHOLIC ACID METABOLITES EXCRETED BY *Rhodococcus jostii* RHA1

by

Kendra Lynn Swain

A THESIS SUBMITTED IN PARTIAL FULFILLMENT OF

THE REQUIREMENTS FOR THE DEGREE OF

MASTER OF SCIENCE

in

THE FACULTY OF GRADUATE STUDIES

(Microbiology and Immunology)

THE UNIVERSITY OF BRITISH COLUMBIA

(Vancouver)

August 2011

© Kendra Lynn Swain, 2011

Abstract

In this study, I investigated two novel transporters associated with cholic acid catabolism in *Rhodococcus jostii* RHA1. Reverse-transcriptase quantitative-PCR indicated that an ABC transporter was upregulated 16.7-fold and an MFS transporter was upregulated 174-fold during the exponential phase of growth on cholic acid compared to pyruvate. With gene knockout analysis, I discovered that these transporters are required for the reassimilation of distinct cholic acid metabolites. The ABC transporter, encoded by the *camABCD* genes, was essential for uptake of 12-hydroxy-9-oxo-1,2,3,4,10,19,23,24-octanorcholan-5,22-dioic acid and 12-hydroxy-9-oxo-1,2,3,4,10,19,23,24-octanorchol-6-en-5,22-dioic acid. The MFS transporter, encoded by the *camM* gene, was essential for uptake of 3,7,12-trihydroxy-9-oxo-9,10-seco-23,24-bisnorchola-1,3,5(10)-trien-22-oic acid. The uptake of these metabolites is necessary for maximal growth on cholic acid: the Δ*cam*B mutant, lacking the permease component of the ABC transporter, and the Δ*cam*M mutant, lacking the MFS transporter, only achieved 74% and 77%, respectively, of the final wild type protein yield. These metabolites differ from previously reported cholic acid metabolites from Proteobacteria in that they retain an isopropionyl side chain at the C17 position. This study is the first to demonstrate the function of putative cholic acid genes through targeted mutagenesis, as well as the first to provide evidence for the requirement for transporters involved in cholic acid metabolite uptake. This work highlights the importance and complexity of transport processes associated with bacterial catabolism and may contribute to industrial applications involving bacterial steroid transformation.

Table of Contents

Abstract ..... **ii**

Table of Contents ..... **iii**

List of Tables ..... **vii**

List of Figures ..... **viii**

Acknowledgements ..... **xi**

Chapter 1: Introduction **1**

1.1 Steroids 1

1.1.1 Steroid Function 1

1.1.2 Steroid Therapeutics 2

1.1.3 Steroids in the Environment 2

1.2 Microbial Steroid Degradation 4

1.2.1 Harnessing Microbial Steroid Catabolic Pathways for Industrial Purposes 4

1.2.2 Steroid Bioremediation using Microorganisms 6

1.3 The Seco-steroid Degradation Pathway 7

1.3.1 Microbial Testosterone Degradation 8

1.3.1.1 17β-Dehydrogenation 10

1.3.1.2 Transformation of Androstenedione 10

1.3.1.3 Transformation of DOHNAA 11

1.3.1.4 Steroid Pathway Gene Clusters in *C. testosteroni* 12

1.3.2 Microbial Cholesterol Degradation 12

1.3.2.1 Modeling *M. tuberculosis* Cholesterol Degradation in *R. jostii* RHA1 12

1.3.2.2 Cholesterol Uptake 13
1.3.2.3 Cholesterol Side-Chain Degradation and A-ring Oxidation 13
1.3.2.4 Predicting Cholesterol Pathway Gene Function 16
1.3.2.5 Rings A and B Degradation and DOHNAA Generation 16
1.3.3 Microbial Bile Salt Degradation 17
1.3.3.1 Bile Salt Degradation by Free-Living Bacteria 18
1.3.3.2 Relevance of Microbial Bile Salt Transformation 19
1.3.3.3 The Unifying Scheme of Microbial Bile Salt Degradation 20
1.3.3.4 Initiation of the Bile Salt Pathway 20
1.3.3.5 -Oxidation of Bile Salts in *Pseudomonas* sp. Strain Chol1 21
1.3.3.6 Degradation of Rings A and B 22
1.4 RHA1: An Excellent System to Study Cholic Acid Catabolism 24
1.4.1 The Unique Properties of Actinobacteria 24
1.4.2 The Resilience of Rhodococci 24
1.4.3 Bile Salt Pathway Genes in RHA1 25
1.4.4 The Aim of this Study 27
Chapter 2: Materials and Methods 29
2.1 Reagents and Chemicals 29
2.2 Cell Growth Assays 29
2.3 DNA Manipulation and Construct Preparation 31
2.4 Cloning of Knockout Mutants 35
2.5 Cloning of Complementation Strains 36
2.6 RNA Extraction 38

2.7 cDNA Synthesis 39
2.8 RT-QPCR Analysis 39
2.9 Chemical Analysis 40
Chapter 3: Results 42
3.1 RHA1 Cholic Acid Growth Phenotype 42
3.1.1 Extracellular Cholic Acid Metabolite Accumulation by RHA1 44
3.2 Expression of the ATP-Binding Cassette and MFS Transporters 45
3.3 Inactivation of the ABC Transporter 48
3.3.1 The Cholic Acid Growth Phenotype of Δ*cam*B 49
3.3.2 Extracellular Cholic Acid Metabolite Accumulation by Δ*cam*B 50
3.3.3 RHA1 and Δ*cam*B Growth on HOONCA Metabolites 54
3.4 Inactivation of the MFS Transporter 55
3.4.1 The Cholic Acid Growth Phenotype of Δ*cam*M 55
3.4.2 Extracellular Cholic Acid Metabolite Accumulation by Δ*cam*M 57
3.4.3 RHA1 and Δ*cam*M Growth on THOSBNC 59
3.5 Cholic Acid Conjugate Growth Phenotype of Δ*cam*M 60
3.6 Complementation 61
Chapter 4: Discussion 63
4.1 Cholic Acid Uptake and the Potential for Passive Diffusion 63
4.2 A Unifying Scheme for Steroid Degradation 64
4.3 Support for the Toxic Metabolite Excretion Hypothesis 65
4.4 Two Novel Transporters 67
4.5 Habitat of Cholic Acid Degraders 67

4.6 Implications..... 68

References..... 70

List of Tables

Table 2.1 Stock salt solution recipe.....30

Table 2.2 Concentrated Goodies recipe.....30

Table 2.3 100X Mg/Ca/B1/Goodies mix recipe.....31

Table 2.4 M9 basal salts recipe for 1L.....31

Table 2.5 Fosmids and plasmids used in this study.....32

Table 2.6 Oligonucleotides used in this study.....34

List of Figures

Figure 1.1 Stucture of the steroid nucleus: cyclopentanoperhydrophenantrene (sterane).....1

Figure 1.2 β-Sitosterol and cholesterol; the two most common starter steroids for whole cell bioconversion.....5

Figure 1.3 Proposed testosterone degradation pathway of *C. testosteroni* TA441.....9

Figure 1.4 Proposed cholesterol side-chain degradation pathway.....14

Figure 1.5 Deduced cholesterol nucleus degradation pathway.....15

Figure 1.6 Structure of cholic acid.....17

Figure 1.7 Proposed β-oxidation of the cholic acid side chain.....21

Figure 1.8 Structure of DHOPDC.....22

Figure 1.9 Structure of DHADD.....22

Figure 1.10 Structure of THSATD.....23

Figure 1.11 ATP-binding cassette transporter.....26

Figure 1.12 Multi-drug transporter of the MFS superfamily.....26

Figure 3.1 Growth of RHA1 on 2.0 mM cholic acid as the sole carbon and energy source..42

Figure 3.2 Final protein assay of all strains grown on 2.0 mM cholic acid.....43

Figure 3.3 Cholic acid metabolite HOONCA.....44

Figure 3.4 Cholic acid metabolite Δ^6-HOONCA.....44

Figure 3.5 Cholic acid metabolite THOSBNC.....45

Figure 3.6 Relative upregulation of *cam*B during growth on cholic acid based on RT-QPCR.....46

Figure 3.7 The ABC-transporter operon genes.....47

Figure 3.8 Relative upregulation of *cam*M during growth on cholic acid based on RT-QPCR.....47

Figure 3.9 Colony PCR electrophoresis gel screening for Δ*cam*B transconjugation.....48

Figure 3.10 Δ*cam*B cholic acid phenotype compared to wild type.....49

Figure 3.11 Accumulation of HOONCA metabolites in wild type RHA1 versus Δ*cam*B, based on GCMS normalized peak abundance.....51

Figure 3.12 Chromatogram of Δ*cam*B stationary phase supernatant showing peaks of accumulated metabolites.....52

Figure 3.13 Mass spectrum of HOONCA.....52

Figure 3.14 Mass spectrum of Δ^6-HOONCA.....53

Figure 3.15 Color-comparison of supernatants.....53

Figure 3.16 Growth of RHA1 and Δ*cam*B on HOONCA metabolites as a carbon and energy source.....54

Figure 3.17 Colony PCR electrophoresis gel screening for Δ*cam*M transconjugation.....55

Figure 3.18 Growth of Δ*cam*M on 2.0 mM cholic acid, compared to wild type measured via OD_{600}.....56

Figure 3.19 Cholic acid growth curve measured as protein.....57

Figure 3.20 THOSBNC accumulation in RHA1 and Δ*cam*M based on normalized GCMS peak abundance.....58

Figure 3.21 Chromatogram of Δ*cam*M stationary phase culture showing peaks of accumulated metabolites.....58

Figure 3.22 Mass Spectrum of THOSBNC.....59

Figure 3.23 Growth of RHA1 and Δ*cam*M on the THOSBNC metabolite as a carbon and energy source.....60

Figure 3.24 Structures of conjugated bile salts.....61

Acknowledgements

I would like to thank my supervisor, Dr. William W. Mohn, for his wisdom, insight, and genuine kindness as he guided me through my journey as a graduate student. Dr. Mohn encouraged me to develop as an independent thinker and a capable scientist.

I thank my committee members, Dr. Erin Gaynor and Dr. Lindsay Eltis, for their intelligent perspective and thoughtful suggestions, as well as their positive affirmations when I was on the right track.

I appreciate my lab members for creating a hard-working, amiable environment that made it a joy to work in our lab. I'd particularly like to thank Justin LeBlanc for training me in RT-QPCR, and for holding my hand through the trials of the SacB protocol. I appreciate Dr. Somalinga Vijayakumar for being there to bounce ideas off of when I needed a second opinion. I especially thank Gordon Stewart for being my "go to" guy for random bits of information, and for all the help he provided me with the GCMS.

I feel very grateful for the help of Jie Liu with all the cloning involved in my project, especially for teaching me her "fool proof" method for designing primers. I also appreciate Dr. Israel Casabon for helping me name the cholic acid metabolites I isolated.

Finally, I'd like to thank Alex Schwartz for believing in me and emotionally supporting me through the most stressful periods of being a graduate student.

Chapter 1: Introduction

1.1 Steroids

Steroids are a class of organic compounds composed of a nucleus of 17 carbon atoms, arranged in 3 cyclohexane rings and a cyclopentane ring fused together, usually referred to as rings A through D (Figure 1.1). Steroids vary in structure by functional groups bound to different sites on this steroid nucleus; there are hundreds of variations found in animals, plants and fungi [1].

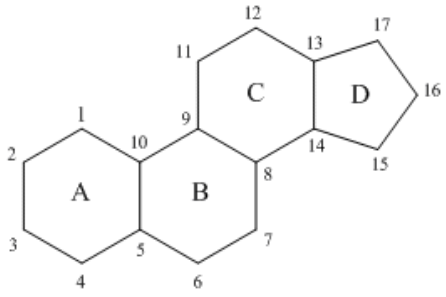


Figure 1.1 Structure of the steroid nucleus: cyclopentanoperhydrophenantrene (sterane).

1.1.1 Steroid Function

Different kinds of steroids perform different functions. Within animals, there are the hormone steroids, which are responsible for sexual differentiation, reproduction, regulation of metabolism, immune function, and muscle and bone synthesis to name a few [2]. As well, cholesterol is a major mammalian steroid responsible for modulating fluidity of cell membranes. Ergosterol in fungi and phytosterols in plants essentially perform the same

membrane function as cholesterol in mammals [3]. There are only a few reports of steroid synthesis in bacteria; including certain methanotrophic bacteria, myxobacteria, and marine bacteria [4].

1.1.2 Steroid Therapeutics

Steroids are also major pharmaceutical compounds. They are routinely prescribed as anti-inflammatory, immunosuppresive, progestational, diuretic, anti-fungal, anabolic and contraceptive agents [1]. Certain steroids have also been used to treat osteoporosis and some forms of breast and prostate cancer, to inhibit HIV-integrase, as well as treat HIV and AIDS [5, 6]. Neurosteroids are those synthesized by glial cells that are present in high concentrations in the central and peripheral nervous system. In a therapeutic context, certain neurosteroids are useful as memory-enhancers, anti-convulsants, and anti-depressants. They have also been shown to have neuroprotective effects against oxidative stress-induced damage, as well as DNA-damage in the brain caused by exposure to mutagens [7]. There is currently an on-going effort to discover new, therapeutically useful steroid compounds, to add to the extant battery of thousands.

1.1.3 Steroids in the Environment

Steroids are released in large quantities in the environment through excretion and decomposition of eukaryotes, as well as in waste from industrial processes [8]. The fate of hormone steroids is potentially the best studied due to the concern for endocrine disruption in

humans, fish and other wildlife. Hormone steroids are released into the environment through human sewage and wastewater treatment, as well as animal waste disposal [9]. Cattle are an especially large source of livestock-generated hormones as they are often given steroids to control ovulation and induce abortion, or fed muscle-building androgens to promote growth [10]. Human females release large quantities of estrogenic steroids when menstruating, or especially while pregnant. Estrogen-like steroids also get released through the urine of females taking contraceptives [11].

The presence of estrogenic steroids is especially problematic in aquatic environments. They have been detected in ground water, surface water, and one study even found an average concentration of 0.7 ng/L of estrogenic steroids in drinking water in the south of Germany [2]. Estrogenic steroid contamination can interrupt egg protein production, and can result in the feminization of freshwater fish, higher levels of phytoestrogens in agricultural crops, as well as harmful effects on the reproductive systems of humans [12, 13]. Aquatic systems downstream of pulp and paper mill effluent have exhibited the masculinization of female fish, indicating the presence of androgenic steroids [14]. The treatment of sewage and industrial waste requires a major improvement to prevent this unfettered release of steroids into the environment. The application of biotechnology is a potentially effective and eco-friendly method to deal with steroid contamination.

1.2 Microbial Steroid Degradation

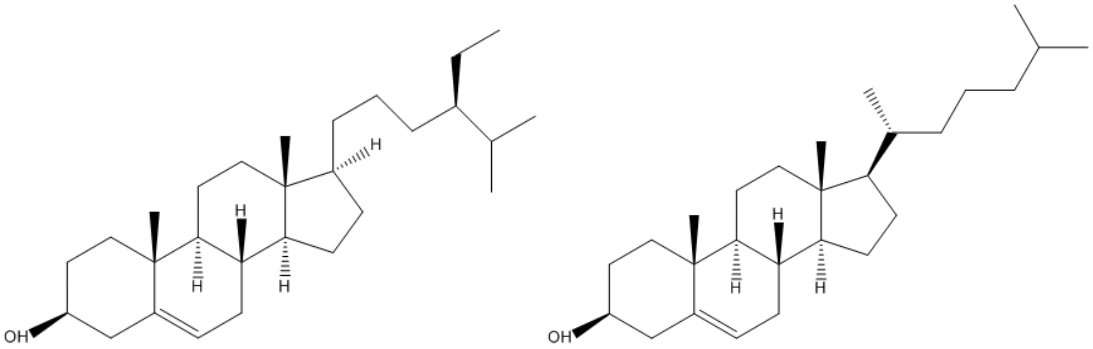
Microorganisms have evolved diverse strategies to uptake, transform and degrade steroid compounds. In the natural environment, microbial steroid degradation is an important part of global carbon cycling. In aerobic environments, microorganisms transform steroids released by eukaryotic excretion or decay into biomass and carbon dioxide [4]. Microorganisms within the human body have also evolved to partly metabolize steroids encountered in the digestive system [3].

1.2.1 Harnessing Microbial Steroid Catabolic Pathways for Industrial Purposes

Highly regio- and stereo-selective reactions are required to produce therapeutically and commercially valuable steroids. These reactions often require extreme conditions, temperatures, and hazardous reagents in order to synthetically produce the desired steroid. The expense and energy requirement of synthetic steroid production has led to the development of some high-yield biological production of steroid therapeutics that requires mild reaction conditions and can be performed without the hazardous reagents required in chemical synthesis. Because biological processes are less energetically costly, they are not only more environmentally friendly but also cheaper than chemical syntheses [15].

Such biotechnology essentially converts a readily available starter steroid into a commercially desirable one by using microorganisms to perform some or all of the transformation reactions. Because of the processing required to isolate, purify, and stabilize enzymes and to regenerate their intermediates, it is more economical to use whole cells for

steroid manufacture [16]. Cholesterol and β-sitosterol (Figure 1.2) are most often used as the raw materials for microbial transformation into C_{17}-ketosteroids, which are then used as the precursors for the synthesis of various steroid drugs [17]. Cholesterol is mainly extracted from animal sources like wool grease, lard or milk fat, yet despite its good properties for microbial transformation, it is more expensive and less widely-available than β-sitosterol, which is extracted from plants [18]. In order to find cheaper raw materials, there is a great interest in using waste products from pulp and paper mills, or vegetable oil production, as sources for starter steroids. For example, Dias, et al. [19] reported the use of steroids harvested from the above waste products as starting materials for transformation by *Mycobacterium* sp NRRL 3805 into androstadienedione, which can then be made into contraceptives and corticosteroids.



β-sitosterol **Cholesterol**

Figure 1.2 β-Sitosterol and cholesterol; the two most common starter steroids for whole cell bioconversion [15].

Research in the field of steroid biocatalysis began around 1950 with the discovery of a *Rhizopus* species capable of performing a crucial step in the synthesis of steroids with useful biological activity [1]. Since then, microbial bioconversion of steroids has been

implemented in the large scale production of natural or modified steroid analogues, focusing mainly on steroid hydroxylation, Δ^1-dehydrogenation, and sterol side-chain cleavage [15]. Production of steroid drugs is one of the most successful applications of microbial technology in large scale industrial processes. However, the power of microbial steroid transformation is not being harnessed to its full extent – only a fraction of the microbial genes and enzymes capable of transforming steroids are well characterized. A more thorough understanding of how bacteria take up and metabolize these compounds is required in order to better exploit microbes in the manufacture of steroids.

1.2.2 Steroid Bioremediation using Microorganisms

Steroid metabolism is also an important aspect of bioremediation. One study by Chevron Petroleum Technology Company examined the effects of landfarming on waste petroleum sludge at Chevron's refinery in Perth Amboy, New Jersey [20]. Landfarming involves mixing contaminated soil with uncontaminated soil, and changing conditions, such as moisture content, aeration and pH, to maximize the rate of contaminant degradation. This study used hydrocarbons indigenous to and ubiquitous in crude oils as biomarkers for the progress of bioremediation. Chief among these biomarkers were steroid hydrocarbons including steranes, monoaromatic and triaromatic steroids, and steroids with the cholestane side chain. They found that even in the most degraded samples, biodegradation of these compounds had proceeded only partially to completion.

Another study by Jacobsen, et al. [21] showed the necessity for viable soil microorganisms to mineralize steroids in a range of conditions, including temperatures, and

soil types. They also noted that the organic amendments brought on by the addition of animal manure altered the pathways and kinetics of steroid dissipation. The effects of animal waste on microbial steroid transformation are relevant in a real-world context, as effluent from sewage treatment plants or agricultural run-off will undoubtedly effect the functioning of the receiving microbial community in soil or water systems. Thus, any bioremediation attempts on animal waste-contaminated sites must take this into account. Oil-contaminated sites, as well as sewage-treatment plant and agricultural effluent, are ideal candidates for "bioaugmentation", i.e. treating the site with natural or genetically engineered bacteria known to catabolize complex hydrocarbons, especially steroid molecules. With more detailed knowledge of the genes and enzymes bacteria use to transform and degrade steroids, more efficient cocktails of bioremediating strains can be created to specifically deal with different kinds of steroid pollution.

1.3 The Seco-steroid Degradation Pathway

The microbial degradation of cholesterol, testosterone, androstenedione and various bile salts has been the subject of intensive study since the 1950s [15]. In the microorganisms studied so far, it has been shown that the degradation pathways of cholesterol, testosterone and the bile acids merge at the generation of 1,4-androstadiene-3,17-dione (ADD) (Figure 1.3, III) and its respective derivatives, which may have variable side chains at C17 and hydroxyl or ketone groups at other positions on the steroid nucleus. The aerobic degradation of ADDs proceeds via the 9,10-seco-pathway, so called because of the generation of steroids with an opened B-ring, which are referred to as "seco-steroids" [22]. The steps leading up to

the generation of ADDs happen differently depending on the starting steroid. The seco-steroid pathway results in the formation of 2-hydroxyhexa-2,4-dienoic acid (2-HHD) (Figure 1.3, VIII) from the former A-ring, and an acidic perhydroindane derivative composed of the former B-ring, and rings C and D, called 9,17-dioxo-1,2,3,4,10,19-hexanorandrostan-5-oic acid (DOHNAA) (Figure 1.3, IX). The further conversion of DOHNAA is still under investigation [23, 24]. Details on what has been elucidated for each steroid's catabolic pathway are discussed separately and in detail in the sections to follow.

1.3.1 Microbial Testosterone Degradation

Comamonas testosteroni is well known for its ability to transform testosterone. The intermediate compounds it generates during testosterone degradation were identified in the 1960s. Guided by these intermediates, the main pathway of testosterone degradation in *C. testosteroni* was predicted (Figure 1.3), and the genes involved in the pathway have been the focus of intensive study ever since [25].

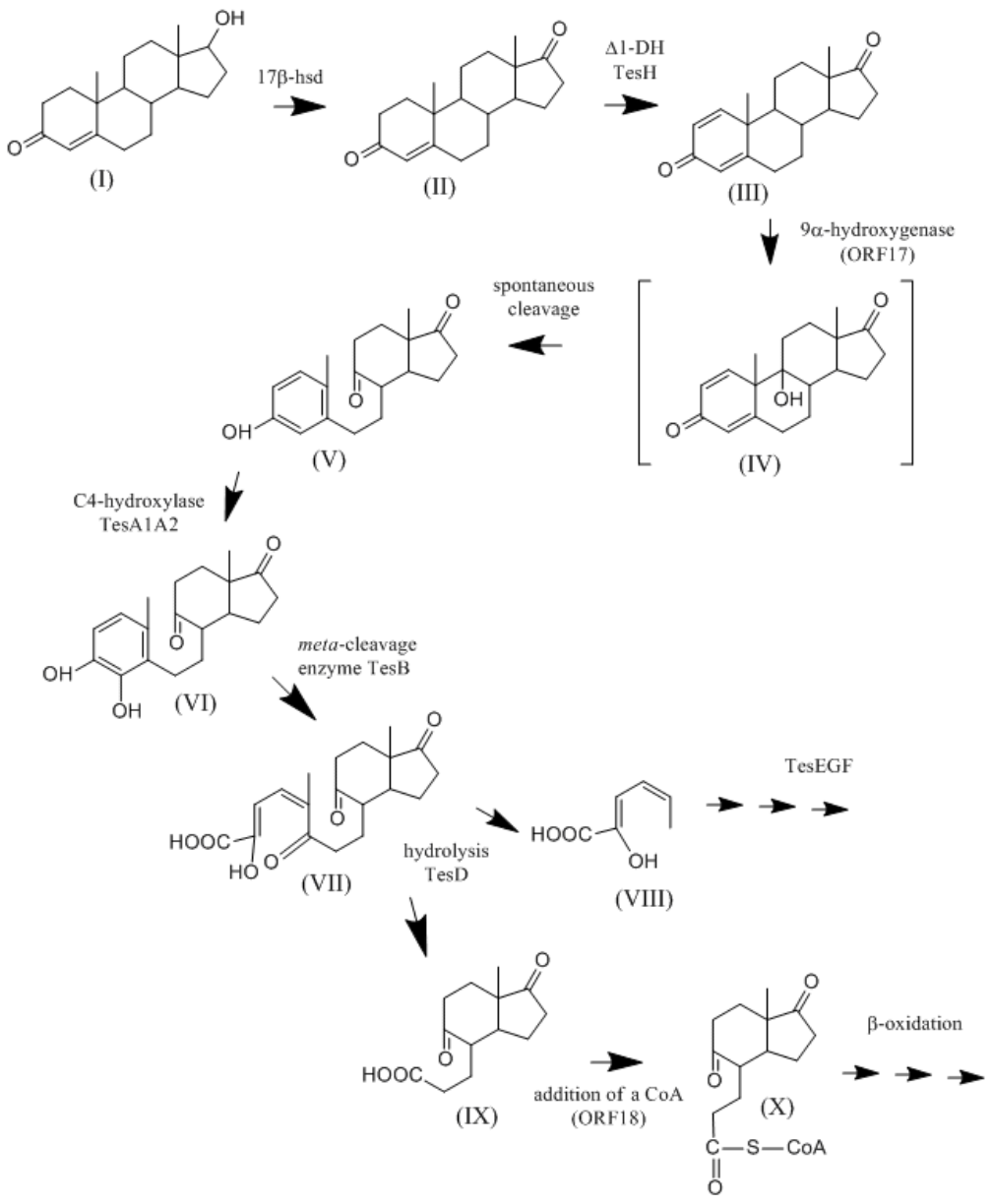


Figure 1.3 Proposed testosterone degradation pathway of *C. testosteroni* TA441. Testosterone, (I); 4-androstenedione (II); androsta-1,4-diene-3,17-dione (III); 9-hydroxyandrosta-1,4-diene-3,17-dione (IV); 3-hydroxy-9,10-secoandrosta-1,3,5(10)-triene-9,17-dione (V); 3,4-dihydroxy-9,10-secoandrosta-1,3,5(10)-triene-9,17-dione (VI); 4,5-9,10-diseco-3-hydroxy-5,9,17-trioxoandrosta-1(10),2-diene-4-oic acid (VII); 2-hydroxyhexa-2,4-dienoic acid (VIII); 9,17-dioxo-1,2,3,4,10,19-hexanorandrostan-5-oic acid (IX); 9,17-dioxo-1,2,3,4,10,19-hexanorandrostan-5-oic acid CoA ester (X) [24]. Multiple arrows indicate more than one enzymatic reaction. Enzymes listed are discussed in detail in the text to follow.

1.3.1.1 17β-Dehydrogenation

The testosterone pathway begins with the initial 17β-dehydrogenation of the hydroxyl group at C17. 17β-Dehydrogenase (17β-HSD) was isolated from *C. testosteroni* TA441 and found to act on both the 3β-hydroxyl and 17β-hydroxyl groups of steroids [26]. A mutant strain of TA441 with a disrupted 17β-HSD gene did not show significant growth on epiandrosterone, which has a 3β-hydroxyl group and a 17-ketone group. However, with noticeably slower growth than wild type, it did degrade testosterone, which has a 17β-hydroxyl and a 3-ketone group (I). Dehydrogenation at the C17 position is thought to be a reversible reaction, as the intermediate compounds isolated with a 17-ketone group are often accompanied by a small amount of analogs with a C17 hydroxyl group. Thus, *C. testosteroni* likely has more than one enzyme capable of 17β-dehydrogenating/hydrogenating activity, while it requires 17β-HSD to degrade 3β-dehydroxy steroids [24]. Therefore, this enzyme might more logically be referred to as 3β-HSD.

1.3.1.2 Transformation of Androstenedione

The dehydrogenation of the 17β-hydroxyl group of testosterone produces 4-androstene-3,17-dione (4-AD) (II). In microbial steroid degradation, a ketone group at C3 and the double bonds, Δ1 and Δ4, are essential for cleavage of the B-ring and aromatization of the A-ring. Δ1-Dehydrogenase (TesH) converts 4-AD to ADD (III) with the insertion of the Δ1 double bond. Subsequently, the oxygenase, 9α-hydroxylase, forms an unstable

intermediate (IV), leading to spontaneous cleavage of ring B between C9 and C10 and aromatization of the A-ring, producing 3-hydroxy-9,10-secoandrosta-1,3,5(10)-triene-9,17-dione (3-HSA) (V). ORF17 is proposed to encode the reductase component of 9α-hydroxylase, because an ORF17-disrupted mutant of strain TA441 accumulates ADD when incubated with testosterone [27].

TesA1A2 hydroxylates 3-HSA at C4 to produce 3,4-dihydroxy-9,10-secoandrosta-1,3,5(10)triene-9,17-dione (3,4-HSA) (VI). 3,4-HSA is then cleaved between C4 and C5 by *meta*-cleavage enzyme TesB to produce 4,5-9,10-diseco-3-hydroxy-5,9,17-trioxoandorosta-1(10),2-diene-4-oic acid (4,9-DHSA) (VII). The hydrolase TesD then hydrolyzes 4,9-DHSA to produce 2-HHD (VIII) and DOHNAA (IX). TesEGF degrade what is left of the A-ring in a process similar to the bacterial degradation of aromatic compounds [24]. ORF18 was shown to be necessary for the further degradation of DOHNAA, as ORF18-disrupted mutants accumulate DOHNAA when incubated with testosterone. Based on database searches, ORF18 was implicated in encoding a CoA-synthetase, suggesting the degradation of DOHNAA is initiated by the addition of CoA (X) [28].

1.3.1.3 Transformation of DOHNAA

Further degradation of DOHNAA has not yet been elucidated, however analysis of intermediates accumulated by gene-disrupted mutants involving the ORF1-33 of strain TA441 suggest degradation is initiated mainly via β-oxidation [24].

1.3.1.4 Steroid Pathway Gene Clusters in *C. testosteroni*

Genes for the degradation of steroid structures make up two major gene clusters in *C. testosteroni*. The first is composed mainly of genes involved in the aromatization and cleavage of the A-ring (named *tesG* to ORF18 in strain TA441) and the second consists of genes involved in the β-oxidation of the B,C,D-rings (named *steA* to *tesR* in strain TA441). Recently these two gene clusters were shown to be several dozens of kilobases apart on the same DNA strand, with quite a few possible steroid degradation genes located in the intervening DNA, suggesting this DNA region of more than 100 kb may be a large steroid degradation gene locus of *C. testosteroni* [29].

1.3.2 Microbial Cholesterol Degradation

Microbial transformation of steroids has recently also received attention from biomedical researchers due to the hypothesis that *Mycobacterium tuberculosis*, the leading cause of mortality from bacterial infection, may use host cholesterol during lung infection [30].

1.3.2.1 Modeling *M. tuberculosis* Cholesterol Degradation in *R. jostii* RHA1

Recent genomic analysis showed that approximately 60% of the 3,999 genes of *M. tuberculosis* are conserved in the related Actinobacterium *Rhodococcus jostii* RHA1, including many genes of unknown function. Because of this genetic similarity, RHA1 has

been used as model organism for the cholesterol catabolic pathway of *M. tuberculosis*, in hopes of shedding light on how *M. tuberculosis* utilizes host cholesterol during infection [23].

1.3.2.2 Cholesterol Uptake

The genome sequence of *M. tuberculosis* revealed four sets of "mammalian cell entry" genes (*mce*), *mce1-4*, which are of particular interest due to their predicted role in pathogenesis [31]. Deletion of nearly the entire *mce3* or *mce4* operon increased long term survival of mice after low dose aerosol infection, and a decreased bacterial burden was also observed in infections with the *mce4* deletion mutants [32]. Based on bioinformatic analysis, it is highly likely that the *mce1* and *mce4* loci encode novel types of ABC transporters. It has been demonstrated that the Mce4 system is involved in steroid transport, and is specifically required for the uptake of cholesterol, 5-α-cholestanol, 5-α-cholestanone, and β-sitosterol; all steroids with similar structures [33]. Thus the cholesterol catabolic pathway of *Rhodococci and Mycobacteria* requires the Mce4 system to transport the steroid into the cell.

1.3.2.3 Cholesterol Side-Chain Degradation and A-ring Oxidation

The microbial degradation of cholesterol involves two processes: side-chain degradation and the degradation of the rings of the steroid nucleus. The order of these events may vary depending on the organism [34]. In RHA1 it was found that oxidation of the side chain precedes oxidation of the 3β-hydroxyl moeity of the A-ring. CYP125 is a steroid 26-

monooxygenase that catalyzes the formation of C26 to the corresponding carboxylic acid, or to an intermediate, to initiate degradation of the side chain (Figure 4) [35, 36]. Further degradation of the side chain proceeds in a process similar to the β-oxidation of fatty acids. Several acyl coenzyme A (CoA)-ligases, dehydrogenases, hydratases and thiolases are thought to catalyze the activation and thiolytic cleavage of the cholesterol side chain. This process releases two propionyl-CoA plus one acetyl-CoA [37]. RHA1 has a series of genes that are upregulated during growth on cholesterol that encode the types of enzymes necessary for this process [23].

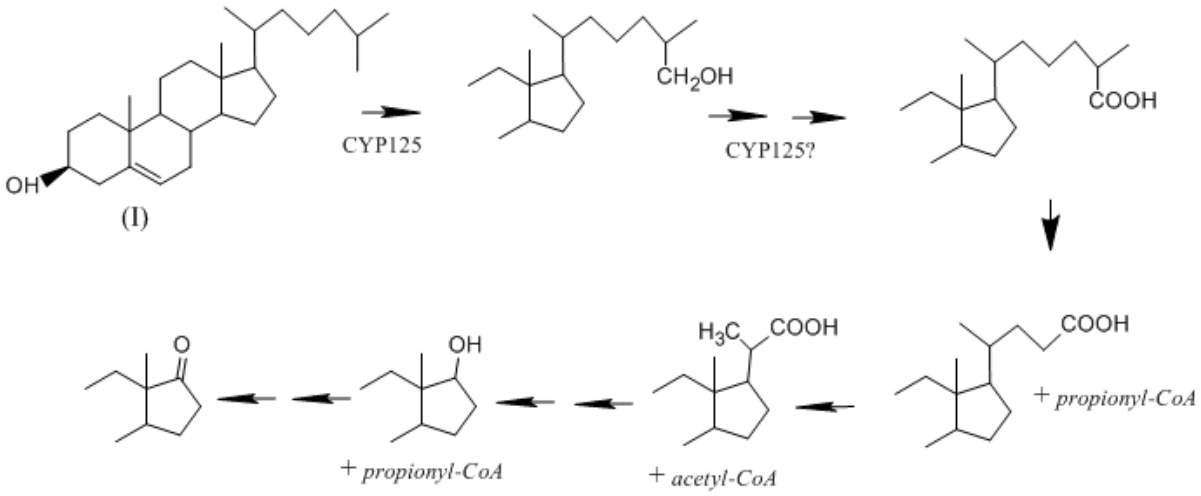


Figure 1.4 Proposed cholesterol (I) side-chain degradation pathway. Double arrows indicate more than one enzymatic reaction.

Depending on the strain, either an O_2-dependent cholesterol oxidase (CHO) or 3β-hydroxysteroid dehydrogenase (3β-HSD) catalyzes the generation of 4-cholestene-3-one by oxidating the 3β-hydroxyl moeity and isomerizing Δ^5 into Δ^4 (Figure 1.5) [35]. Accumulation

of 4-AD (II) and ADD (III) has been detected in some mutants of *Mycobacterium* sp. suggesting that further side-chain degradation occurs before appreciable degradation of the steroid rings. However, in certain RHA1 mutants, accumulations of 3-HSA with a C17 isopropyl side chain were detected, thus in certain strains, the order of the degradation of the side chain and rings may vary [37].

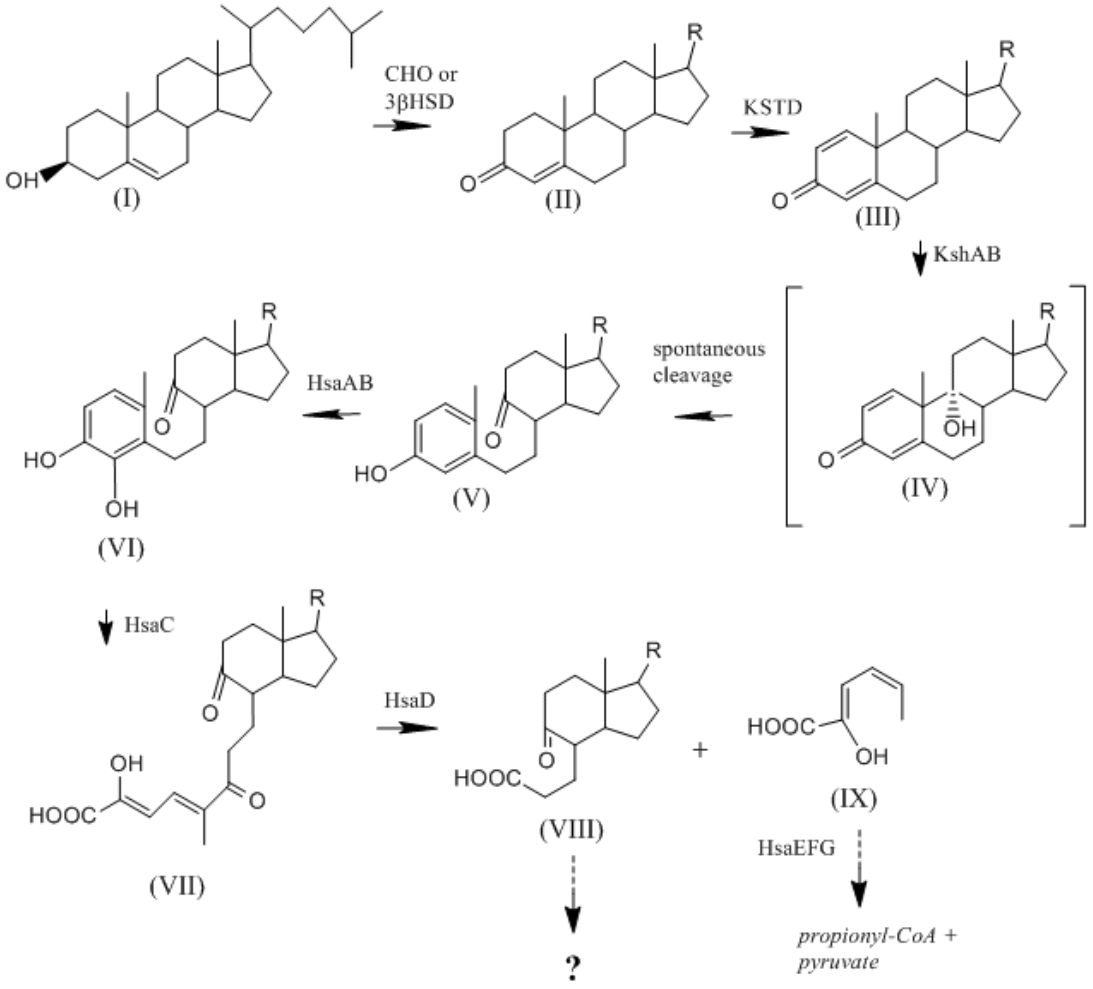


Figure 1.5 Deduced cholesterol nucleus degradation pathway. Cholesterol, (I); AD (II); ADD (III); 9OHADD (IV); 3-HSA (V); 3,4-DHSA (VI); 4,9-DHSA (VII); DOHNAA (VIII); 2-HHD (IX). Dashed arrows indicate multiple enzymatic steps. The C17 side-chain is represented as R as the progress of side-chain degradation with regards to ring oxidation may vary depending on the strain.

1.3.2.4 Predicting Cholesterol Pathway Gene Function

A recent study by van der Geize, et al. [23] found that during growth of RHA1 on 2 mM cholesterol, 572 genes were variously upregulated when compared to growth on pyruvate. A cluster of 51 genes was found to encode proteins that have significant sequence identity with already-characterized enzymes involved in the catabolism of rings A and B in strain TA441 and *Rhodococcus erythropolis* SQ1, such that the function of several of these RHA1 enzymes can be confidently predicted.

1.3.2.5 Rings A and B Degradation and DOHNAA Generation

KSTD, a 3-ketosteroid Δ^1-dehydrogenase, performs the Δ^1-dehydrogenation of C1, generating ADD or a derivative with a partial side-chain (III) [38]. KshAB, encoding a two component 3-ketosteroid 9α-monooxygenase, introduces the 9α-hydroxyl moeity into the B-ring, generating 9α-hydroxy-4-androstene-3,17-dione (9OHADD) (IV) [39]. This allows for the nonenzymatic hydrolysis of 9OHADD into 3-HSA (V). The enzymes KSTD, KshA and KshB of RHA1 are 40-69% identical to their orthologs identified in *R. erythropolis* SQ1 [23].

Further degradation of 3-HSA by RHA1 is thought to proceed in the same manner as observed in testosterone degradation by strain TA441. Seven genes, with names beginning with *hsa* are clustered with *kstD* and *kshA* on the RHA1 genome, encoding proteins that share 30-60% amino acid sequence similarity with orthologs encoded by *tes* genes of strain TA441 [27, 40]. HsaAB, a 2-component, flavin-dependent monooxygenase, hydroxylates ring A of 3-HSA at C4 yielding 3,4-DHSA (VI). HsaC, an extradiol dioxygenase, cleaves 3,4-DHSA

to produce 4,9-DHSA (VII). HsaD then hydrolyzes the C5-C6 bond to produce DOHNAA (VIII) and 2-HHD (IX). 2-HHD is further transformed by HsaEFG, a hydratase, an aldolase and an acetaldehyde dehydrogenase respectively, to propionyl-CoA and pyruvate. As in the testosterone pathway of *C. testosteroni*, the further degradation of DOHNAA in RHA1 and *M. tuberculosis* is still being investigated [37].

1.3.3 Microbial Bile Salt Degradation

Bile acids are surface active steroids that aid in the digestion of dietary fats in vertebrates [41]. They are highly water-soluble, due to the α-hydroxyl groups at C3, C7 and C12, as well as the five-carbon acyl side chain attached to C17 (Figure 6). Because all the hydroxyl groups protrude in the same direction, bile acids are amphiphilic and act as detergents. As such, bile acids can perturb the structure of the bacterial cell membrane and induce lysis [42].

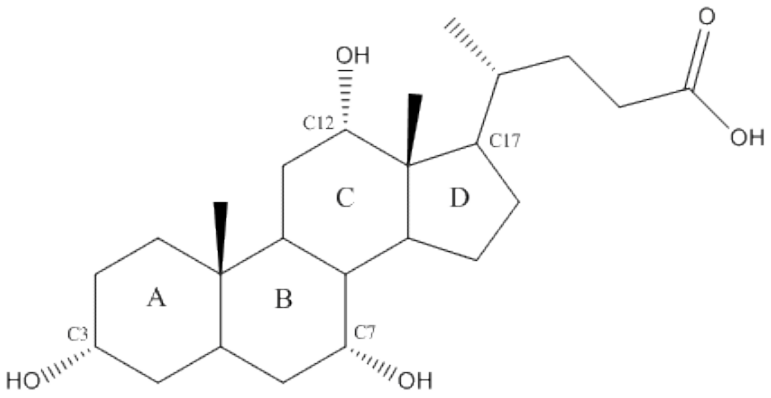


Figure 1.6 Structure of cholic acid.

Bile salts are bile acids with a cation, usually sodium, on the hydroxyl group of the C17 side chain. The ability to degrade bile salts is widespread amongst bacteria, and is well-studied in anaerobic bacteria of the intestines [4]. Enteric bacteria have evolved diverse physiological adaptations to deal with high concentrations of bile salt: in the duodenum, bacteria face bile salt concentrations of up to 20 mM [43]. Intestinal bile salt transformation is mainly achieved by anaerobic bacteria of the genera Bacteroides, Eubacterium and Clostridium. The benefit of bile salt transformation for intestinal bacteria seems to be the acquisition of glycine and taurine from conjugated bile salts [43, 44].

1.3.3.1 Bile Salt Degradation by Free-Living Bacteria

Considerable quantities of bile salts are released into the environment through fecal matter (300 – 600 mg per day per human) and urine (approximately 4 mg per day per human) [22]. Thus, it is not surprising that many aerobic soil and aquatic bacteria can grow with bile salts as a carbon and energy source. Complete aerobic degradation of bile salts has been reported by various groups of bacteria from Actinobacteria, Betaproteobacteria and Gammaproteobacteria. The best studied bile salt degrading Actinobacteria are members of the genera, *Arthrobacter, Corynebacterium*, *Mycobacterium, Nocardia, Rhodococcus,* and *Streptomyces [16]*. Of the Betaproteobacteria, *C. testosteroni* is being intensively studied, and of the Gammaproteobacteria, different *Pseudomonas* species are of interest [4, 24].

For free-living bacteria, bile salts are both a nutrient source and a potential stress factor. For *Pseudomonas* sp. strain Chol1, it was shown that seco-steroids produced in the degradation pathway have toxic effects. Thus, these microorganisms have likely evolved

adaptive strategies to reduce their exposure to toxic bile acid degradation products. One possibility is that the degradation pathway proceeds in such a manner so as to reduce the cell's exposure to toxic substrates. Several studies support this hypothesis by showing the transient extracellular accumulation of degradation intermediates, which would keep intracellular levels of these toxic compounds low [45]. It is not yet known whether accumulation of these metabolites is the product of diffusion or of active efflux, however efflux systems for non-charged steroids have been found, and a bile salt exporter has been postulated for intestinal bacteria [43]. Transient extracellular accumulation of bile salt degradation products also implies uptake of these intermediates for further conversion, but currently no intermediate uptake systems have been characterized [45].

1.3.3.2 Relevance of Microbial Bile Salt Transformation

For energy conservation, free-living bacteria generally appear to oxidize bile salts completely to CO_2, thus bile salt degradation is relevant as a source of atmospheric CO_2 [4]. Bacterial bile salt transformation also has applications in biotechnology, as bile salts and their precursors are processed to their desired conformation by biotransformation to be used as treatment for gallstones [46]. Another goal is to develop probiotic strains for introduction to the intestines that transform certain conformations of bile salts, thereby lowering the concentration of secondary bile salts that are presumptive colon cancer promoters [43]. Finally, the pathway for bile salt degradation merges with that of other steroid substrates, such that knowledge of bile salt metabolism is relevant for metabolic engineering of steroid-transforming bacteria in general [4].

1.3.3.3 The Unifying Scheme of Microbial Bile Salt Degradation

In 1982, Hayakawa proposed a unifying scheme for bacterial bile salt degradation based on investigations from the 1970s and 1980s that detected intermediates in bacterial cultures growing on bile salts [22]. However, most of what is known about the actual pathway is based on degradation pathways for other steroids. The differentiation of the degradation pathway of cholic acid, the primary mammalian bile salt, from that of testosterone or cholesterol is the processing of the 3α-,7α-, and 12α-hydroxyl groups and the acyl-side chain.

1.3.3.4 Initiation of the Bile Salt Pathway

As with other steroids, the hydroxyl group at C3 must be oxidized to a ketone before the desaturation of the A-ring can occur via double bond insertion between C1 - C2 and C4 - C5. Because the C3 hydroxyl group is in the α-orientation as opposed to β, as seen in cholesterol and testosterone, it potentially requires a different HSD than the aforementioned steroids. Degradation of the side-chain begins with activation of the acyl-group by Coenzyme A (CoA; Figure 1.7). Formation of cholyl-CoA was detected in strain Chol1, as well as formation of CoA-esters of 3-ketocholate and $\Delta^{1,4}$-3-ketocholate. Thus it is still unclear whether CoA activation happens before or after A-ring oxidation; like the cholesterol degradation pathway, the order in which these events occur likely varies from strain to strain, or possibly happens simultaneously [4].

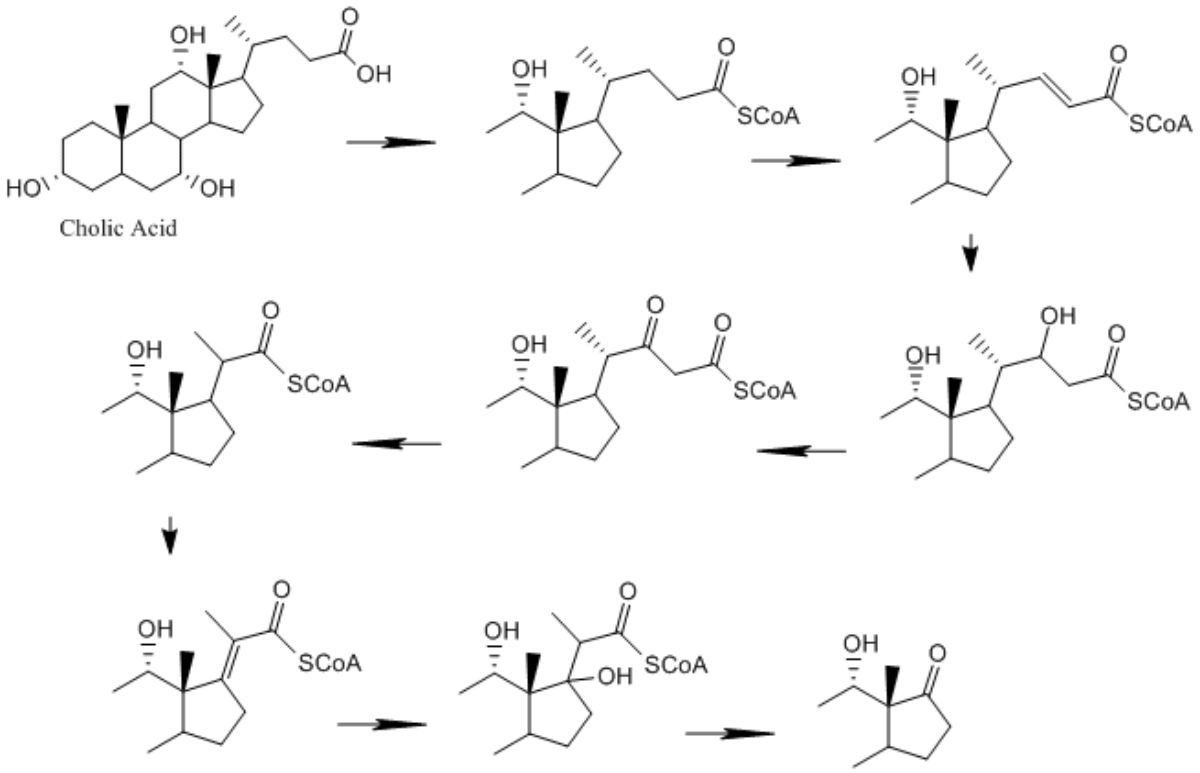


Figure 1.7 Proposed β-oxidation of the cholic acid side chain [45].

1.3.3.5 β-Oxidation of Bile Salts in *Pseudomonas* sp. Strain Chol1

Birkenmaier, et al. [45] did the first genetic and biochemical study on the β-oxidation of bile salts. They created the R1 transposon mutant of strain Chol1, with a disrupted *acad* gene, that accumulates the compound 7α,12α-dihydroxy-3-oxopregna-1,4-diene-20-carboxylate (DHOPDC; Figure 1.8), which is similar to AD but has a 7α-hydroxyl and a 12α-hydroxyl group, and an isopropionyl side chain. The *acad* gene encodes a putative acyl-CoA-dehydrogenase, which inserts a double bond into the side chain of DHOPDC-CoA. Accumulation of DHOPDC has also been detected in a mutant of strain TA441 with a

transposon inserted in a gene with 70% similarity to strain Chol1's *acad* [45]. The compounds that have been identified as intermediates in cholic acid degradation support the proposed pathway that proceeds via β-oxidation of the side chain [4].

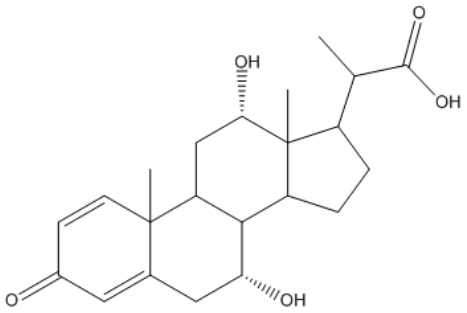


Figure 1.8 Structure of DHOPDC [45].

1.3.3.6 Degradation of Rings A and B

β-Oxidation of the side chain leads to the formation of 7,12-dihydroxy-1,4-androsteine-3,17-dione, or DHADD (Figure 1.9).

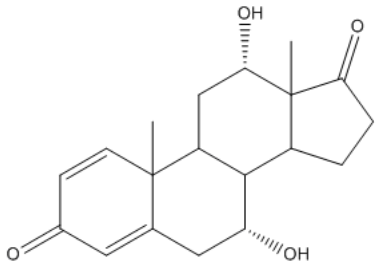


Figure 1.9 Structure of DHADD [45].

In strain TA441, it is postulated that the 12α-hydroxyl group sterically hinders 9α-hydroxylase from binding C9, thus it must first be converted to the β-orientation so a 9α-hydroxyl can be added to the B ring [24]. Then, opening of ring B and the aromatization of ring A results in the formation of 3,7,12-trihydroxy-9,10-secoandrosta-1,3,5(10)triene-9,17-dione (THSATD) (Figure 1.10).

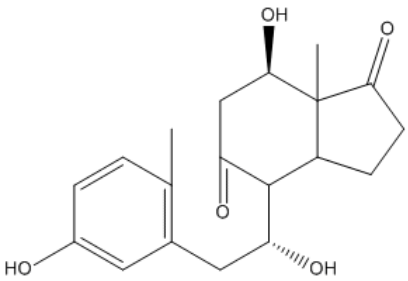


Figure 1.10 Structure of THSATD [45].

During incubations of strain Chol1 with cholic acid, it was found that in the first half of exponential grown, all of the cholic acid was converted to THSATD, which accumulated in the medium and was then degraded in the second half of exponential growth [45]. The rest of the unifying scheme for cholic acid degradation follows the seco-steroid degradation pathway that is observed in testosterone and cholesterol, complete with generation of 2-HHD and 7,12-dihydroxy DOHNAA [4], with the exception that the hydroxyl groups at C7 and C12 are not modified during the above degradation process.

In order to shed light on the unique intricacies of microbial cholic acid degradation and how it differs from that of testosterone or cholesterol, detailed studies of the genes and

enzymes involved in the pathway are required. In addition, understanding the mechanisms behind the observed efflux and uptake of intermediates can be crucial in a biotechnological context.

1.4 RHA1: An Excellent System to Study Cholic Acid Catabolism

1.4.1 The Unique Properties of Actinobacteria

The Actinobacteria are a group of high-GC, gram-positive bacteria that are ubiquitous in diverse environments. In soil, Actinobacteria provide essential ecosystem services, decomposing and recycling numerous organic compounds [47]. Potentially the most important features of Actinobacteria in determining their ecological niches and fitness are their catabolic versatility and ability to withstand environmental stresses. These capacities at least partially explain the large genomes typical of soil Actinobacteria, as exemplified in RHA1. This soil Actinomycete boasts a large, fully-sequenced 9.7-Mb genome, packed with genes that allow it to catabolize a wide range of aromatic compounds, including carbohydrates, nitriles, steroids, and xenobiotic compounds as sole sources of carbon and energy [48].

1.4.2 The Resilience of Rhodococci

The cell wall of rhodococci is composed of mycolic acids, similar to those found in *Mycobacterium*. Mycolic acids contain long aliphatic chains that facilitate the uptake and

subsequent metabolism of hydrophobic substrates across the cell envelope [49]. Rhodococci can survive in starvation conditions and in many cases, the degradation of pollutants is not repressed in the presence of more easily degradable carbon sources [50]. These attributes make rhodocci highly suitable for environmental remediation. Because they grow rapidly and robustly on a wide variety of substrates, they are highly useful in biotechnological applications in the pharmaceutical and chemical industries, primarily for biotransformation and biodegradation of organic compounds [51]. Likewise, they are good candidates for the industrial production of bioactive steroid compounds, but we must first understand more about the mechanisms rhodococci use to transform steroids [15].

1.4.3 Bile Salt Pathway Genes in RHA1

RHA1 is an excellent system to study microbial steroid catabolism. The genome of RHA1 appears to encode at least four distinct steroid catabolic pathways. Microarray analysis of this organism grown separately on cholesterol, androstenedione, and cholic acid revealed over 700 genes that were variously upregulated on these three steroids (*Mohn, W.W., et al. unpublished*). Guided by this transcriptomic analysis, research focused on cholesterol degradation has identified several genes in RHA1 involved in cholesterol uptake, side-chain removal, and initial ring degradation [33, 48]. A homologous yet distinct degradation pathway for cholic acid catabolism is also implicated by the transcriptomic data. Several genes are upregulated that are likely involved in the degradation of the cholic acid side chain, and rings A and B. In addition to pathway genes, genes encoding an ATP-binding cassette (ABC) transporter (ro04888 – ro04885, Figure 1.11) and a multi-drug transporter of

the MFS superfamily (ro05792, Figure 1.12) are also highly upregulated by RHA1 growing on cholic acid. The ABC transporter appears to include an individual permease and ATP-binding components as well as a fused permease/ATP binding component.

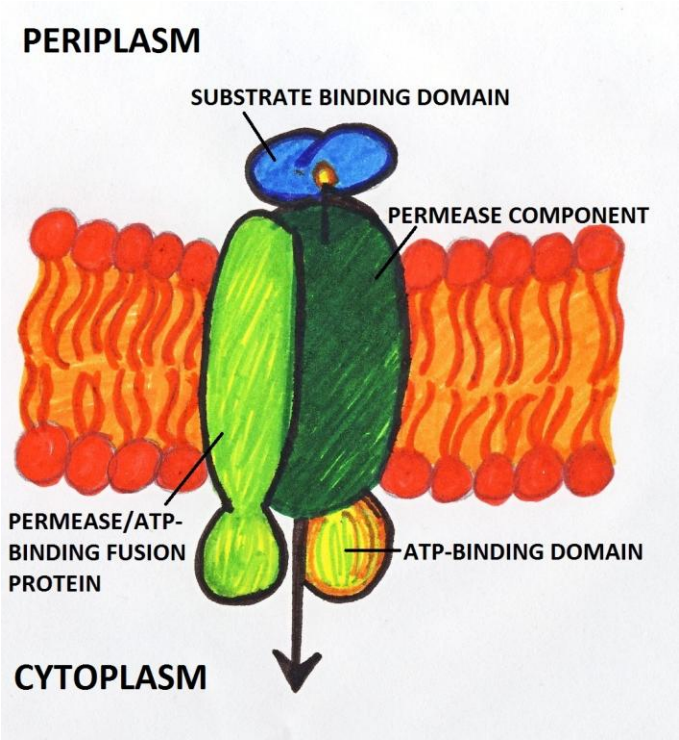


Figure 1.11 ATP-binding cassette transporter.

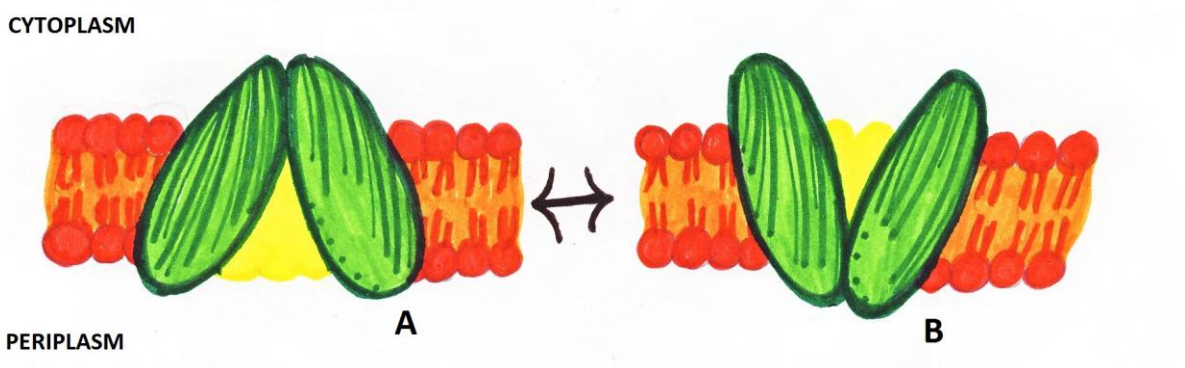


Figure 1.12 Multi-drug transporter of the MFS superfamily: A. outward-facing conformation, B. inward-facing conformation.

1.4.4 The Aim of this Study

This study examined two transporters associated with cholic acid catabolism. Knockout mutants of RHA1 were generated in which the above ABC and MFS transporters were individually inactivated using unmarked, in-frame gene deletion. Growth of the wild-type and mutant strains on cholic acid was characterized, and metabolite production was determined. Like other organisms grown on cholic acid, RHA1 also exhibits the transient accumulation of extracellular metabolites, which are reassimilated and further degraded in later exponential and stationary growth phase. Neither transporter was required for uptake of cholic acid, but each was essential for the assimilation of particular metabolites, which were structurally elucidated.

To our knowledge, this is the first study to identify and characterize transporters required for the assimilation of excreted steroid metabolites. Preliminary structural analysis suggests these extracellular metabolites are very structurally similar to those that accumulate in studies of other organisms grown on cholic acid [4, 45], except that the THSATD-derivative of RHA1 retains an isopropyl-side chain at C17. This implies that RHA1 also degrades cholic acid via the same pathway as previously characterized gram-negative bacteria, but that RHA1 differs with respect to the order of nucleus and side chain degradation.

This study contributes to the knowledge of the bacterial physiology behind certain steroid transformations, as well as demonstrates that during microbial cholic acid catabolism, A-ring oxidation, cleavage of the B-ring, and potentially even generation of 7,12-dihydroxy-

DOHNAA, can precede complete degradation of the C17 side chain in some strains. In addition, this study sheds new light on the diversity of functions that transport proteins can perform. Finally, this research contributes to the fundamental knowledge of the physiology, genetics, and ecology of the industrially and environmentally important members of *Rhodococcus* and related genera.

Chapter 2: Materials and Methods

2.1 Reagents and Chemicals

All reagents and chemicals were ordered from Fisher Scientific, Sigma, Bio Rad, Thermo Scientific, and Invitrogen and used without further purification unless specified. Cholic acid was at minimum 98% pure. Restriction Enzymes for cloning were purchased from New England Biolabs. T4 DNA ligase was purchased from Fermentas. Water for media preparation and experimental procedures was purified to a resistivity greater than 10 MΩ·cm using a Thorton 200CR Conductivity/Resistivity Instrument from Mettler Toledo.

2.2 Cell Growth Assays

RHA1 and derivative strains were cultivated at 30°C and 200 rpm in M9 mineral medium [52] supplemented with Goodies [53]. This is composed by creating a stock salt solution (Table 2.1), adding 50 ml of the stock salts to 100 ml total of a concentrated Goodies solution (Table 2.2), adding 75 ml of this concentrated Goodies solution to 300 ml total of a Mg/Ca/B1/Goodies mix (Table 2.3) and finally combining 1 ml of this Goodies mix with 10 ml of the M9 basal salts solution (Table 2.4), and bringing the volume to 100 mL with H_2O. For a carbon source, either 2.0 mM steroid substrate or 20 mM pyruvate was added.

Escherichia coli strains were grown at 37°C in Luria-Bertani (LB) broth. Bacto agar (1.5% w/v) from Difco was used for solid medium. Culture growth was measured as the

change in optical density at 600 nm. Biomass measurements, based on protein measurements, were performed with a BCA protein assay from Thermo, Scientific, using bovine serum albumin as the standard. To test for transformation of cholic acid metabolites, M9 mineral medium was diluted one-fold with filter-sterilized strain Δ*cam*B or Δ*cam*M culture supernatant harvested during early stationary growth phase.

Table 2.1 Stock salt solution recipe.

Chemical	**g/L**
$MgCl_2$-$6H_2O$	22.94
$CaCO_3$	2.0
$FeSO_4$-$7H_2O$	4.5
$ZnSO_4$-$7H_2O$	1.44
$MnSO_4$-H_2O	0.85
$CuSO_4$-$5H_2O$	0.25
$CoCl_2$-$6H_2O$	0.24
H_3BO_3	0.06
HCl	51.3 mL

Table 2.2 Concentrated goodies recipe (100 mL).

Component	**Quantity**
Stock Salt Solution	50 mL
$MgSO_4$	3.009 g
1% $FeSO_4$	25 mL
H_2O	Adjust volume to 100 mL

Table 2.3 100X Mg/Ca/B1/Goodies mix recipe (300 mL).

Component	Quantity
$MgSO_4$	60 mL
$CaCl_2$	3 mL
10 mM thiamine (vitamin B1)	3 mL
Concentrated Goodies	75 mL
H_2O	Adjust volume to 300 mL

Table 2.4 M9 basal salts recipe for 1 L.

Chemical	Quantity
KH2PO4	30 g
Na2HPO4	60 g
NaCl	5 g
NH4Cl	10 g

2.3 DNA Manipulation and Construct Preparation

DNA was amplified, purified, and manipulated according to standard procedures [52]. Polymerase chain reactions (PCR) were performed with Taq Polymerase from Qiagen or High-Fidelity Expand Polymerase from Roche in a 96-well PTC-200 Peltier Thermal Cycler. Oligonucleotides were designed with GeneRunner software and synthesized at the Nucleic Acid Protein Services Unit at UBC (NAPS). Nucleotide sequencing of clones and constructs were also performed at NAPS.

The mutant strains, Δ*cam*B and Δ*cam*M, were generated, based on previously described methods, by amplifying 800 – 1000 bp fragments that flank the gene of interest, with less than 20% of the targeted gene included in the amplicons [38]. The Δ*cam*B and Δ*cam*M upstream flanking regions were amplified from fosmid DNA (RF00110B17 and

RF00110H09, respectively; Table 2.5) with the following primers: cBupFor, cBupRev, cMupFor and cMupRev (Table 2.6). The downstream flanking regions were amplified in a similar fashion using cBdwFor, cBdwRev, cMdwFor, cMdwRev primers (Table 2.6). Triple-ligations using T4 DNA ligase, with the cut sites for EcoR1, HindIII and SphI for *cam*B and EcoRI, HindIII and XbaI for *cam*M, were performed to clone the amplicons into pK18*mobSac*B (Table 2.5) to produce pK18camB and pK18camM respectively. The mutagenic constructs were transformed by electroporation and propagated in DH5α *E. coli*, chosen for its high transformation efficiency. Time constants of 4.5 volts or higher were achieved for all transformations via electroporation.

Table 2.5 Fosmids and plasmids used in this study.

Fosmids/Plasmids	Relevant characteristics[a]	Reference/origin
RF00110B17	Amp^r	[48]
RF00110H09	Amp^r	[48]
pK18mobSacB	Cm^rKan^r	[54]
pK18camB	Cm^rKan^r, pk18mobSacB *cam*B deletion plasmid	This study
pK18camM	Cm^rKan^r, pk18mobSacB *cam*M deletion plasmid	This study
pSET152	Am^r, int $^{\phi\text{-C31}}$	[55]
pSTcamB	Am^r, int $^{\phi\text{-C31}}$, pSET152 *cam*B complementation plasmid	This study
pSTcamM	Am^r, $int^{phi\text{-C31}}$, pSET152 *cam*M complementation plasmid	This study
pTIP	Amp^rCm^r	[56]
pTIPcamB	Amp^rCm^r, pTIP *cam*B complementation plasmid	This study

[a] Amp^r: ampicillin resistance, Cm^r: chloramphenicol resistance, Kan^r: kanamycin resistance, Am^r: apramycin resistance, int $^{\phi\text{-C31}}$: bacteriophage ϕ-C31 attachment site.

For the complementation assay, primers were designed to include in the amplicons at least 200 base pairs upstream of the target gene or target operon, thereby including the native promoter region. The *cam*B and *cam*M amplicons for the complementation assay were

produced from fosmid DNA (RF00110B17 and RF00110H09, respectively; Table 2.5), using primers camBpSTf and camBpSTr for *cam*B and camMpSTf and camMpSTr for *cam*M (Table 2.6).

DH5α transformants were screened using colony PCR. Colonies were sampled with a toothpick, suspended in 12.5 μl of water with 50 μg/ml proteinase K, incubated at 50°C for 30 minutes and 80°C for 20 minutes, and then centrifuged at 16,000 x g for 5 minutes to remove cell debris. Colony PCR reactions contained 2 μl of the above cell extract, in a total volume of 10 μl. Successful DH5α transformants were grown for 16 hours at 37°C in LB, and their plasmid constructs were then isolated using the Bio Rad plasmid miniprep kit for subsequent transformations.

Table 2.6 Oligonucleotides used in this study.

Primer name	Sequence (5' to 3')[a]	Restriction Site
cBupFor	GCGAAGCTTCGAGATGAAGACGATGTTGTAGCG	EcoRI
cBupRev	CGGGAATTCGCGCAGAACAAGATCCTCTCGTTC	HindIII
cBdwFor	CGGAAGCTTGCGGTCTTCGTGGTCCTCATC	HindIII
cBdwRev	GCGGCATGCACCCACCGAGGAGGCCAGTACC	SphI
cMupFor	TCTGAATTCGGTAGTGGACGAGGGTGGCGAC	EcoRI
cMupRev	TTATCTAGAGGGATTCGAGAGGATCAGCACG	XbaI
cMdwFor	TGTTCTAGACTCCTCATCCGCAACAAGATCGAG	Xba1
cMdwRev	TCCAAGCTTCTTTCGACGTGGTCCTCAGCG	HindIII
camBColF	GACGACCAGCGCGAGGATGCAG	---
camBColR	GTCGAAACCCGGAGACGAGGCGTAC	---
camMColF	ACCAGTAGGGCGCGATCTGATGGAG	---
camMColR	AGGTGACCCGGCGCGTCAATC	---
camBpSTf	ATATCTAGAAGACACGTTCGCCGAGTCGGTC	XbaI
camBpSTr	AATTCTAGAAGATGTTCGCCAAGACCATCG	XbaI
camMpSTf	AAAGAATTCAGACTGAGTGATTCCGTCATGGG	EcoRI
camMpSTr	AAATCTAGATGAACACTTGGACTGCCACACCG	XbaI
camBpTIPf	CTTGTTACATATGACCATCGTCTGGTCGGGCCTC	NdeI
camBpTIPr	ATCAAGCTTTCACACCACCCGTTCCCGCACC	HindIII
camBQFor	TCTCGTCCCACACGTTCAAC	---
camBQRev	CGAAGGTTCCGACCATCATC	---
camMQFor	CCGTCGCGAAAACATTGG	---
camMQRev	GGATCGGTCATCACGAACATC	---

[a] The indicated restriction enzyme cut sites are underlined.

The construct pTIPcamB (Table 2.5) was generated by amplifying a wild type copy of *cam*B with the camBpTIPf and camBpTIPr primers (Table 2.6). A double-ligation was used to clone this amplicon into pTIP cut with both NdeI and HindIII, and the pTIPcamB construct was then directly transformed into electrocompetent Δ*cam*B cells via electroporation using previously described methods [57].

2.4 Cloning of Knockout Mutants

Gene deletion mutants Δ*cam*B and Δ*cam*M were generated by the previously described *sacB* counterselection system [38]. Wild Type RHA1 was cultivated in Lysogeny Broth Peptone media (LBP) containing 30 μg/ml nalidixic acid at 30°C for 48 hours at 200 rpm. These cultures were then plated on solid LBP agar containing 30 μg/ml nalidixic acid and incubated at 30°C for an additional 48 hours. The mutagenic constructs pK18camB and pK18camM were transformed by electroporation into *E. coli* S17-1 donor cells, which were plated on LBP plates containing 25 μg/ml kanamycin and grown for 24 hours at 37°C, then left at room temperature for an additional 24 hours to garner more cell material. Cells from both the donor strain and the RHA1 plates were suspended in 2 ml of LBP media, and aliquots of 750 μl each were gently mixed together. The cells were pelleted by centrifugation (9,400 x g for 1 min), re-suspended in 1 ml of LBP media, and aliquots of 200 μl were spread on non-selective LBP plates and incubated overnight at 30°C to facilitate conjugation. Cells were then harvested from plates with confluent growth, suspended in 2 ml of LBP media, and aliquots of 100 μl were spread on selective LBP plates with 50 μg/ml kanamycin plus 30 μg/ml naladixic acid and incubated at 30°C for 96 hours.

To initiate the integration of the pK18*mobsac*B construct into the RHA1 genome, kanamycin-resistant colonies were selected and replica-plated on LBP with 10% (w/v) sucrose and on LBP with 50 μg/ml kanamycin, each additionally containing 30 μg/ml nalidixic acid. Within two days, colonies that were sucrose sensitive and kanamycin resistant (Kan^r/Suc^s) were selected and cultured overnight in 25 ml LBP medium at 30°C. Aliquots of 25 μl were spread on LBP plates supplemented with 10% sucrose, and incubated at 30°C for 72 hours. Sucrose resistant colonies were replica-plated on LBP plates as well as LBP supplemented with 50 μg/ml kanamycin. Kanamycin sensitive colonies (Kan^s) were screened by colony PCR using camBColF and camBColR for the *cam*B deletion and camMColF and camMColR for the *cam*M deletion (Table 2.6). The regions of deletion in strains Δ*cam*B and Δ*cam*M were sequenced to ensure there were no changes in the regions flanking the DNA-deletion.

2.5 Cloning of Complementation Strains

The entire 5-kb, four-gene operon *cam*ABCD and the 1.8-kb single-gene *cam*M were cloned to generate the complementation strains Δ*cam*Bc and Δ*cam*Mc. Double-ligations using T4 DNA ligase with the cut sites XbaI for Δ*cam*Bc and EcoRI and XbaI for Δ*cam*Mc were performed to clone the amplicons into the pSET152 integrative vector, to produce pSTcamB for *cam*B complementation and pSTcamM for *cam*M complementation (Table 2.5). XbaI was used to cut both ends of the *cam*B amplicon because it was the only restriction enzyme in the pSET152 multiple cloning site that was also a non-cutter in the

*cam*B operon. The complementation constructs were transformed via electroporation into DH5α *E.coli*.

The mutants Δ*cam*B and Δ*cam*M were individually cultivated in LB media containing 30 μg/ml nalidixic acid at 30°C for 48 hours at 200 rpm. These cultures were then plated on solid LBagar containing 30 μg/ml nalidixic acid and incubated at 30°C for an additional 48 hours. The complementation constructs pSTcamB and pSTcamM were transformed by electroporation into *E. coli* S17-1 donor cells and plated on LB plates containing 50 μg/ml apramycin and grown for 24 hours at 37°C, then left at room temperature for an additional 24 hours to garner more cell material. Cells from both the donor strain and the RHA1 plates were re-suspended in 2 ml of LB media, and aliquots of 750 μl each were gently mixed together. The cells were pelleted by centrifugation (9,400 x g for 1 min), re-suspended in 1 ml of LB media, and aliquots of 200 μl were spread on non-selective LB plates and incubated overnight at 30°C to facilitate conjugation. Cells were then harvested from plates with confluent growth, suspended in 2 ml of LB media, and aliquots of 100 μl were spread on selective LB plates with 50 μg/ml apramycin plus 30 μg/ml nalidixic acid and incubated at 30°C for 96 hours to facilitate integration in the ϕ-C31 bacteriophage attachment site. Subsequent colonies were re-plated on selective LB plates with 50 μg/ml apramycin plus 30 μg/ml nalidixic acid and incubated at 30°C for 48 hours, then screened for the presence of both the truncated and the wild type target gene using cBupFor and cBdwRev primers for Δ*cam*Bc and cMupFor and cMdwRev primers for Δ*cam*Mc (Table 2.6). The pSET152 vector cannot exist freely in *Rhodococcus* strains [55].

Preliminary attempts were made to complement the Δ*cam*B mutant using the inducible expression vector pTIP as previously described [56]. This approach was soon abandoned due to unreliable results, and the pSET152 method was adopted instead.

2.6 RNA Extraction

Samples of 10 ml were taken when cultures reached approximately 35%, 65% and 100% of their maximal OD_{600}., corresponding to exponential, late exponential and stationary phases, respectively. A 1/10 volume of stop solution (95% reagent alcohol: 5% acid phenol [v/v] , pH 5) was added to samples, which were then centrifuged at 4,000 x g and 4°C for 10 minutes. Cells were suspended in 1.0 ml supernatant plus 2.0 ml of RNA Protect from Qiagen, incubated for 5 minutes at room temperature, then centrifuged at 18,000 x g for 2 minutes. Pellets were frozen on dry ice and stored at -80°C. RNA extraction and purification were performed based on previous methods [58] with the following modifications. RNA was isolated from cell pellets by vortexing with glass beads in hot phenol plus sodium dodecyl sulfate at final concentrations of 14.3% and 0.9%, respectively. Cell debris was removed with acetate plus phenol-chloroform [1:1, v/v]. Nucleic acids were precipitated with 0.6 M acetate plus 100% isopropanol, and treated with DNase I from Invitrogen, then incubated at 37°C for 1 hour with RNase Out from Invitrogen. RNA was extracted and precipitated with phenol-chloroform [1:1, v/v], then purified with the Qiagen RNeasy minikit, according to instructions.

2.7 cDNA Synthesis

Synthesis of cDNA was performed with the commercially available ThermoScript™ RT-PCR System protocol from Invitrogen. All reagents were provided from Invitrogen unless otherwise indicated. 5 μg RNA were incubated with 50 ng of random hexamers and 10 mM dNTP Mix. The mixture was brought to 12 μl with diethyl pyrocarbonate (DEPC)-treated water, and incubated at 65°C for 5 minutes, then cooled on ice for 10 minutes. The following mix was prepared and added to each reaction: 5X cDNA Synthesis Buffer, 0.1 M DTT, 10 U RNaseOUT™, 15 U ThermoScript™ RT, brought to 10 μl with DEPC-treated water. The samples were incubated at 25°C for 10 minutes, 50°C for 50 minutes, then 85°C for 5 minutes. 2 U of RNase H was added and the samples were incubated at 37°C for 20 minutes. Fresh cDNA samples were used immediately for RT-QPCR analysis.

2.8 RT-QPCR Analysis

Reverse-transcriptase quantitative PCR (RT-QPCR) measured the expression of targeted genes compared to that of an internal standard gene, ro01702, encoding a DNA polymerase IV. Previous microarray experiments showed that this housekeeping gene is expressed as an approximately constant fraction of total mRNA under a variety of growth conditions and during all growth phases [58]. The TaqMan probes and primers used in this study were designed with the Primer Express Software v2.0 from Applied Biosystems. Each QPCR reaction mixture contained 1.0 μl of the 20 μl of cDNA produced, 200 nM TaqMan probe, and 10 μl 2X TaqMan universal PCR master mix from Applied Biosystems, in a total

volume of 20 μl. Duplicate singleplex reactions for the housekeeping gene and the target gene were performed in a Stratagene Mx3000P real-time PCR system for 2 minutes at 50°C, 10 minutes at 95°C and then 40 cycles of 15 seconds at 95°C and 1 minute at 60°C. The quantitative PCR cycle threshold (C_T) results were analyzed using the comparative C_T method ($\Delta\Delta C_T$ method). The Student's one-sample *t* test was used to evaluate whether the gene targets were differentially regulated. The expression ratios were calculated with the formula $E^{-\Delta\Delta CT}$, where *E* is the average amplification efficiency derived from the standard curves for the target and housekeeping genes [59].

2.9 Chemical Analysis

For gas chromatography mass spectrometry (GCMS) analysis, samples were periodically collected and cells were removed by centrifugation. The supernatant was then acidified with a 1/50 volume 10% H_2SO_4, extracted twice by mixing at room temperature for 30 minutes with an equal volume of ethyl acetate, dried under nitrogen and dissolved in 200 μl pyridine. An internal standard of 0.25 mM cholestane was used to normalize each sample.

The extracts were derivatized at room temperature with 200 μl bis(trimethylsilyl)trifluoroacetamide/trimethylchlorosilane (99:1) from Sigma-Aldrich and analyzed with an Agilent 6890N chromatograph equipped with an HP-5ms capillary column (50 m by 0.25 mm) and a mass-selective detector [60].

The gas chromatogram conditions were as follows: the injector temperature was set at 280°C, the transfer line temperature was 290°C, and the flow rate was 1 ml/min with helium. The temperature program of the oven was 104°C for two minutes, and then increased to

290°C at a rate of 15°C per minute, then held at 290°C for 15 minutes. The mass spec conditions were set to electron emission scanning at 40 – 800 m/z, at 1.97 scans per second.

Chapter 3: Results

3.1 RHA1 Cholic Acid Growth Phenotype

RHA1 was grown in M9 mineral medium with 2.0 mM cholic acid as the sole carbon and energy source as described in section 2.2. After a lag phase of roughly 24 hours, RHA1 achieved a specific growth rate of 0.105 h^{-1} (a doubling time of 2.867 h). At approximately 52 hours, RHA1 reached a maximal OD_{600} of 1.76 ± 0.02 (Figure 3.1) and a final growth yield of 17.4 ± 0.3 μg of protein per 1 ml of culture (Figure 3.2).

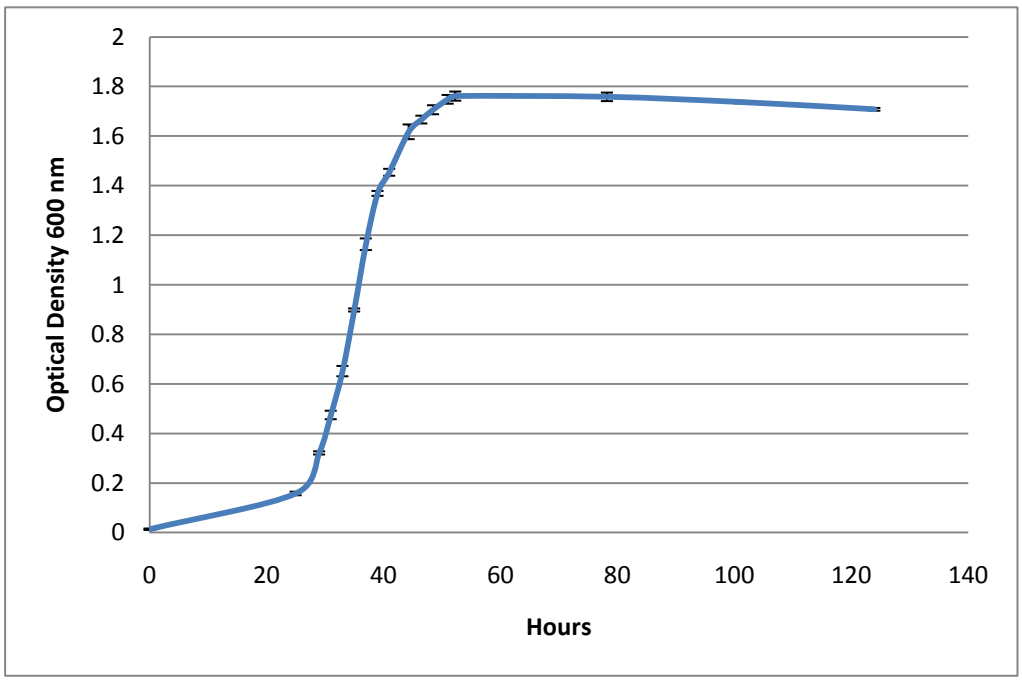


Figure 3.1 Growth of RHA1 on 2.0 mM cholic acid as the sole carbon and energy source; n=3; error bars show standard deviation.

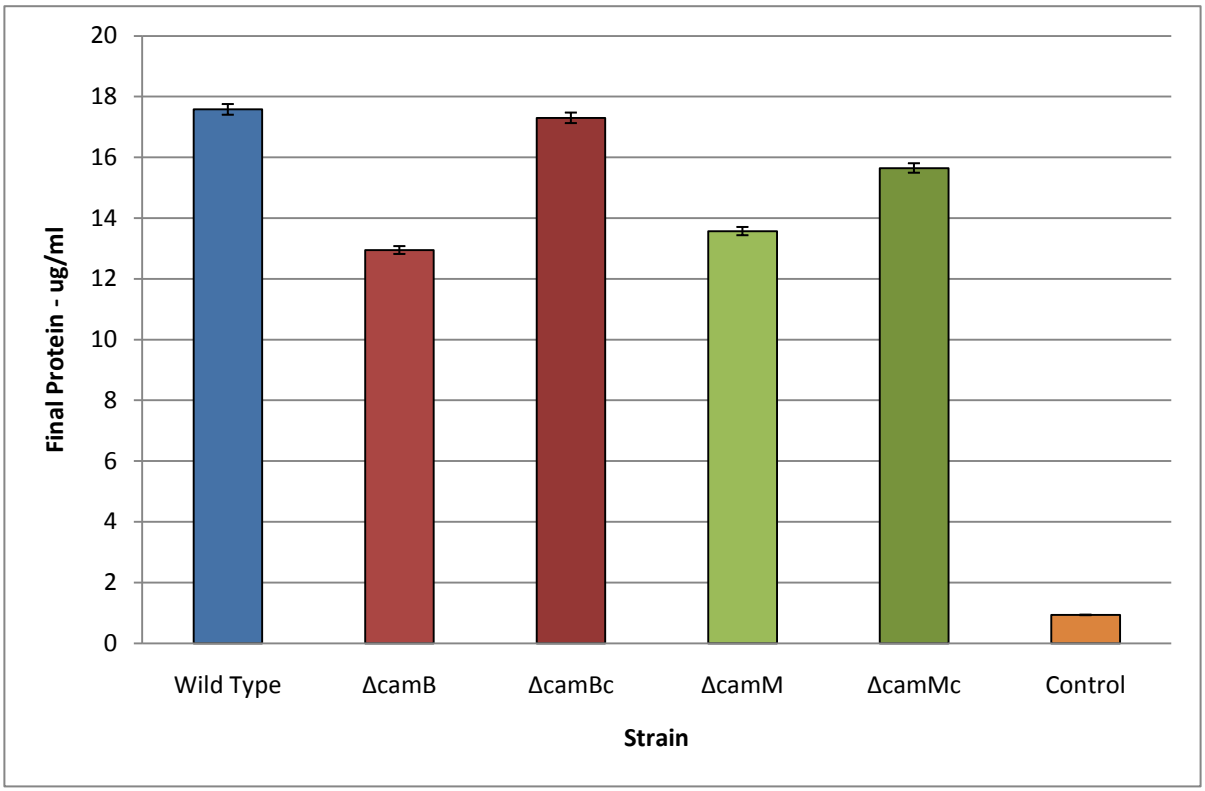


Figure 3.2 Final protein yield of all strains grown on 2.0 mM cholic acid, control was without inoculum; n=3; error bars indicate standard deviation.

RHA1 was grown on 0.2 mM, 2.0 mM, and 5.0 mM cholic acid, in M9 mineral medium, to assess the effect of cholic acid concentration on growth kinetics. With 0.2 mM, compared to 2.0 mM, cholic acid, RHA1 had a shortened lag phase of 15 hours but grew to a lower final OD_{600} of 0.30 ± 0.02. The 5.0 mM cholic acid cultures failed to grow (data not shown), presumably due to toxicity of cholic acid. Thus, it was determined that 2.0 mM is the optimal experimental concentration for RHA1 to achieve maximal growth on cholic acid.

3.1.1 Extracellular Cholic Acid Metabolite Accumulation by RHA1

Three main cholic acid metabolites were detected using GCMS analysis: 12-hydroxy-9-oxo-1,2,3,4,10,19,23,24-octanorcholan-5,22-dioic acid (HOONCA) (Figure 3.3), 12-hydroxy-9-oxo-1,2,3,4,10,19,23,24-octanorchol-6-en-5,22-dioic acid (Δ^6-HOONCA) (Figure 3.4), and 3,7,12-trihydroxy-9-oxo-9,10-seco-23,24-bisnorchola-1,3,5(10)-trien-22-oic acid (THOSBNC) (Figure 3.5). At roughly 36 hours after inoculation, these compounds reached their maximum level of accumulation in the supernatant, corresponding an estimated 12.5%, 4%, and 3%, respectively, of the initial cholic acid added (0.816 g/L), based on the gas chromatogram peak areas.

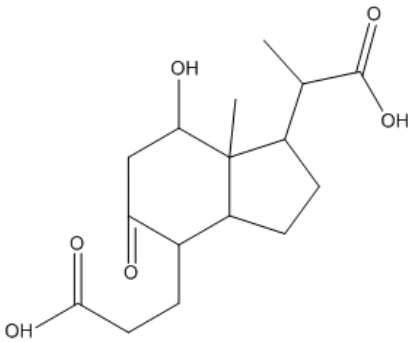


Figure 3.3 Cholic acid metabolite HOONCA.

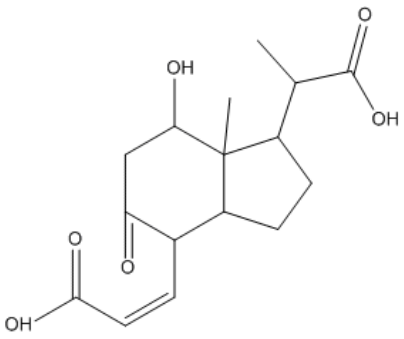


Figure 3.4 Cholic acid metabolite Δ^6-HOONCA.

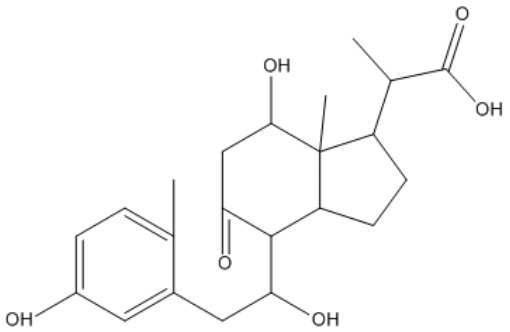


Figure 3.5 Cholic acid metabolite THOSBNC.

By 45 hours post-inoculation, less than half of the above compounds were still present in the supernatant of wild type RHA1, and by late stationary phase these compounds were completely reassimilated and are no longer present in the supernatant. Other metabolites were also found to transiently accumulate in the supernatant, yet they were in such low abundances compared to the above compounds, that they were only considered minor metabolites.

3.2 Expression of the ATP-Binding Cassette and MFS Transporters

In a previous study, transcriptomic analysis of RHA1 was performed in which many genes were found to be upregulated during exponential growth on cholic acid, compared to growth on pyruvate (*W.W. Mohn, unpublished*). Among these upregulated genes were genes encoding two transporters: a four-gene operon encoding an ATP-binding cassette (ABC) transporter, CamABCD (ro04888 – ro04885), and a major facilitator superfamily (MFS) transporter, CamM (ro05792). The prefix, Cam, signifies Cholic acid metabolite transporter. The transcriptomic data revealed that during mid-log phase, the gene encoding a permease component of the ABC-transporter (*cam*B) exhibited 7.4-fold upregulation, and the MFS

transporter gene (*cam*M) showed 26.6-fold upregulation, when RHA1 was grown on cholic acid compared to pyruvate.

To verify upregulation indicated by the transcriptomic data, RT-QPCR was performed on *cam*B as well as *cam*M. The *cam*B gene was most highly upregulated during early log phase, with a normalized 16.7-fold change in transcription, then still upregulated but to a lesser extent in late log phase with an 8.9-fold change in transcription. By early stationary phase, RHA1 grown on cholic acid exhibited almost no difference in levels of transcription of *cam*B compared to RHA1 grown on pyruvate (Figure 3.6).

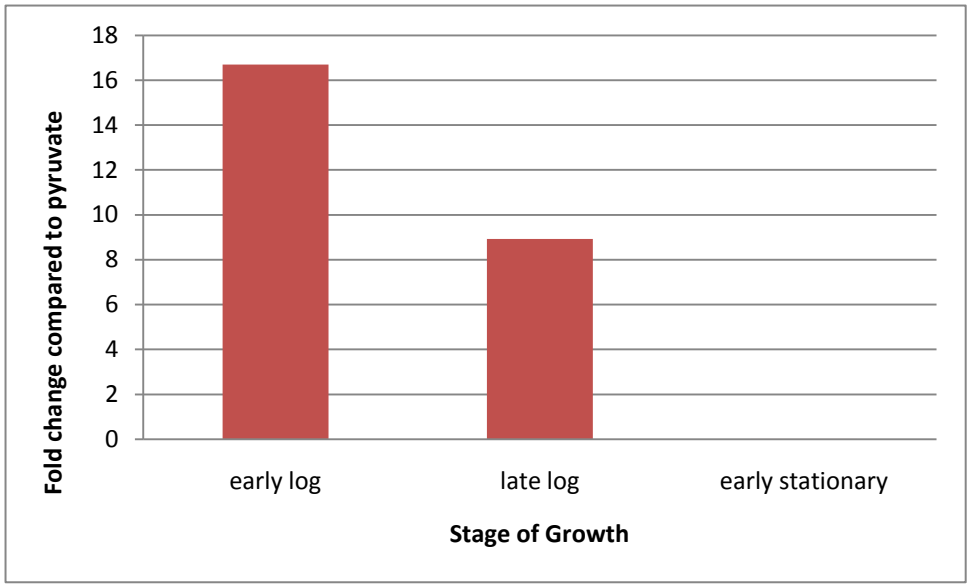


Figure 3.6 Relative upregulation of *cam*B during growth on cholic acid based on RT-QPCR.



Figure 3.7 The ABC-transporter operon genes: *cam*A, substrate binding domain; *cam*B, permease component; *cam*C, fused permease/ATP-binding domain; *cam*D, ATP-binding domain, the arrow indications the direction of transcription.

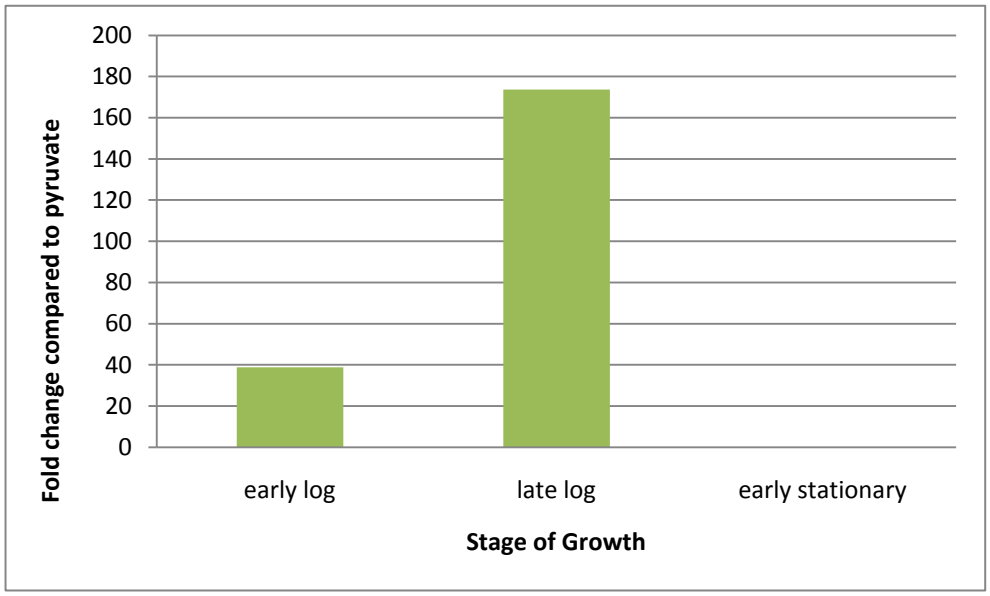


Figure 3.8 Relative upregulation of *cam*M during growth on cholic acid based on RT-QPCR.

Levels of *cam*M transcription were 38.83-fold and 173.7-fold higher during early log and late log phase, respectively, for RHA1 grown on cholic acid compared to pyruvate. Again, during early stationary phase, there was almost no difference in transcription levels of *cam*M between RHA1 grown on cholic acid and pyruvate (Figure 3.8). These RT-QPCR data

confirm that both transport systems are significantly upregulated when RHA1 is grown on cholic acid, suggesting that they are important for cholic acid catabolism.

3.3 Inactivation of the ABC Transporter

CamABCD was inactivated by in-frame deletion of *camB* as described in section 2.4 (Figure 3.9). The permease gene was selected for deletion, as it is the best way to ensure that a single gene deletion inactivates the ABC transporter. The substrate-binding domain and ATP-binding domains of ABC transporters have been found to be somewhat "promiscuous" and can function with other ABC transport systems [61].

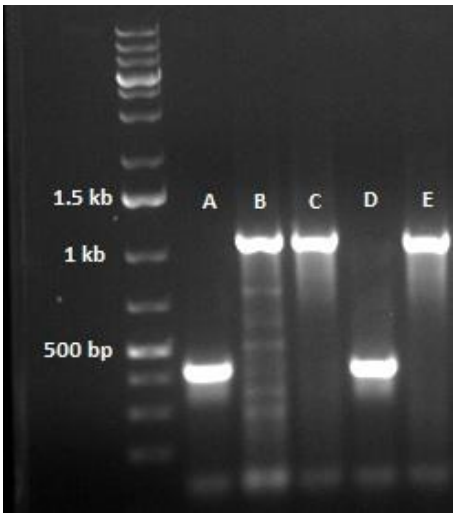


Figure 3.9 Colony PCR electrophoresis gel screening for Δ*cam*B transconjugation: the clones represented in lanes A and D have a truncated copy of *cam*B (480 base pairs), lanes B, C and E have a wild type copy (1000 base pairs), the lane D clone was selected for subsequent growth experiments.

3.3.1 The Cholic Acid Growth Phenotype of Δ*cam*B

The Δ*cam*B mutant was grown on 2.0 mM cholic acid in the same conditions as the wild type. Like wild-type RHA1, Δ*cam*B exhibited an initial lag phase of 24 hours, followed by exponential growth in which the strain achieved a specific growth rate of 0.094 h^{-1} with a doubling time of 3.20 hours. The Δ*cam*B mutant reached a maximum OD_{600} of 1.47 ± 0.01 at 41 hours after inoculation, and then dropped to 1.40 ± 0.02 and slowly decreased in OD_{600} until late stationary phase (Figure 3.10). The final protein yield of Δ*cam*B was 12.9 ± 0.02 μg/ml, which is 74% of the final protein yield of wild type RHA1 (Figure 3.2). Thus, growth kinetics of the mutant were very similar to the wild-type, but the final cell yield was lower.

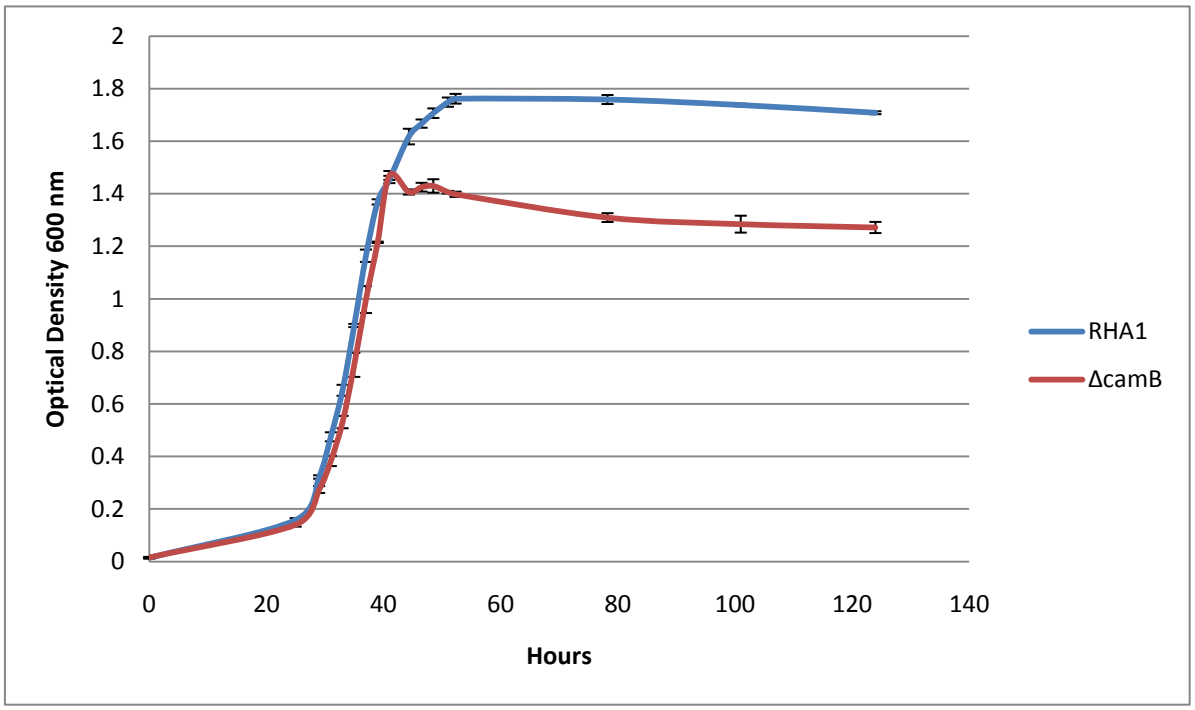
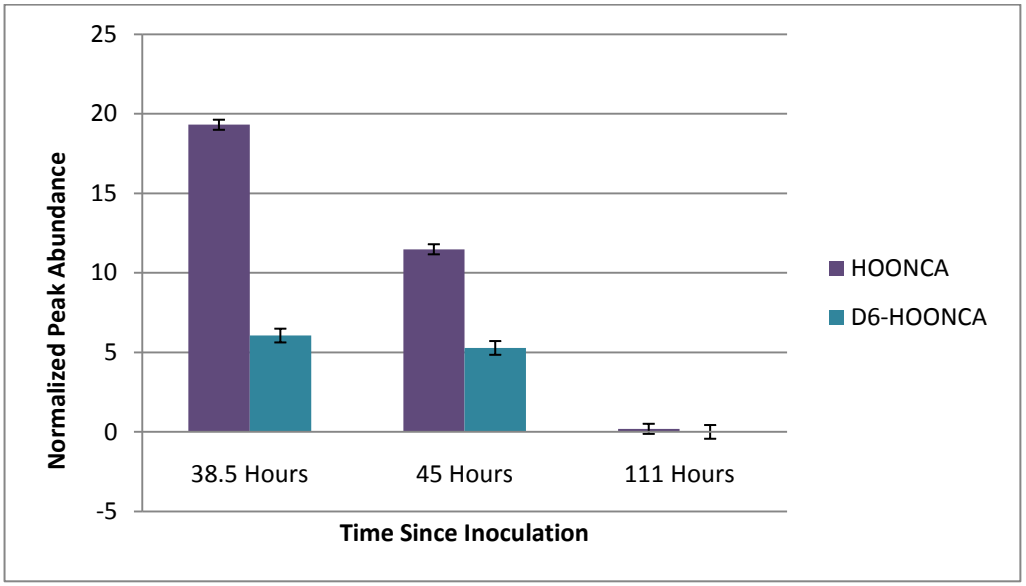


Figure 3.10 Δ*cam*B cholic acid growth phenotype compared to wild type; n=3; error bars indicate standard deviation.

3.3.2 Extracellular Cholic Acid Metabolite Accumulation by Δ*cam*B

Extracellular metabolites were extracted from Δ*cam*B cultures at various times, and it was found that this mutant strain accumulates the same metabolites as wild type. However, unlike wild type RHA1, Δ*cam*B was unable to reassimilate two of these metabolites: HOONCA (Figure 3.3) and Δ^6-HOONCA (Figure 3.4). The maximum accumulation of these HOONCA metabolites roughly corresponds to the point of maximum growth of Δ*cam*B, just after 40 hours (Figure 3.11). These metabolites were identified by their retention time (Figure 3.12), fragmentation pattern, and molecular ion (3.13 and 3.14), as detected by the GCMS, which were consistent over repeated experiments. The structures were determined based on studies of other cholic acid metabolizing microorganisms [45], as well as structures identified in studies of RHA1 grown on cholesterol [23].

A.



B.

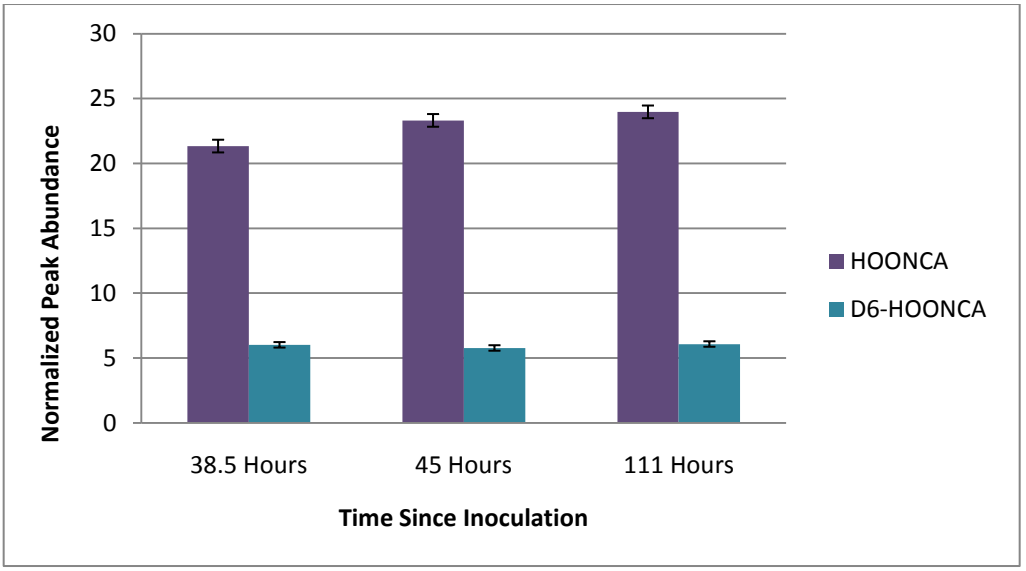


Figure 3.11 Accumulation of HOONCA metabolites in (A) wild type RHA1 versus (B) Δ*cam*B, based on GCMS normalized peak abundance; n=3; error bars indicate standard deviation.

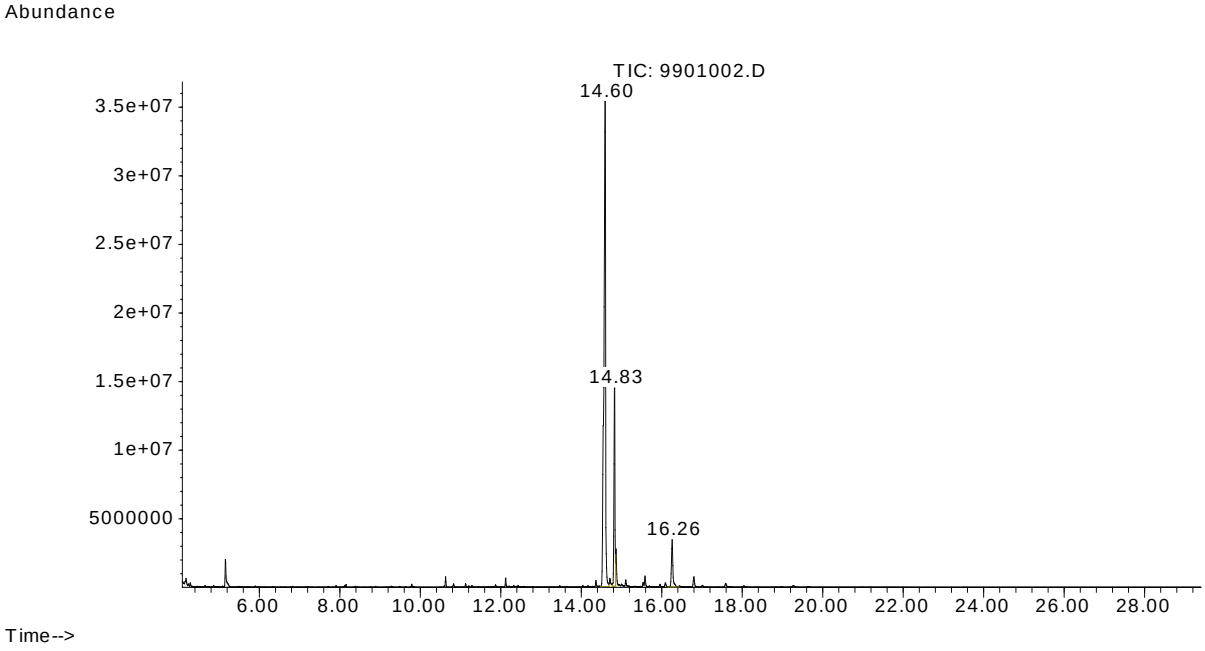


Figure 3.12 Chromatogram of Δ*cam*B stationary phase supernatant showing peaks of accumulated metabolites. Rt 14.60: HOONCA, rt 14.83: Δ^6-HOONCA, rt 16.26: cholestane internal standard.

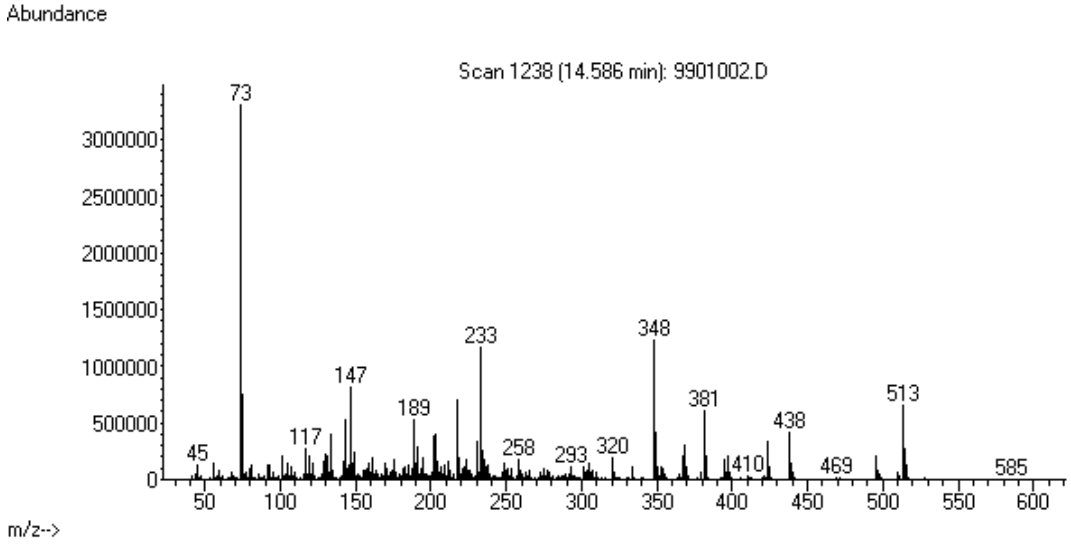


Figure 3.13 Mass spectrum of HOONCA.

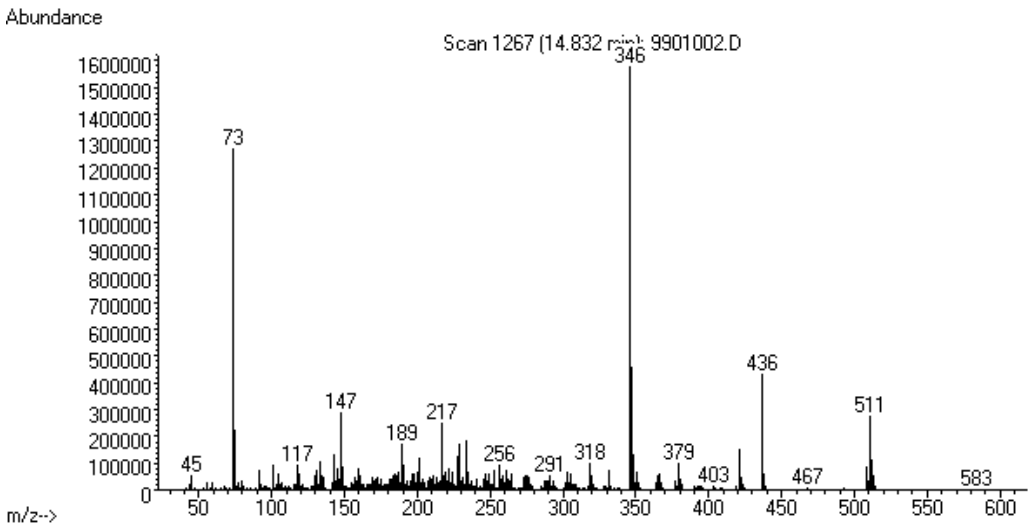


Figure 3.14 Mass spectrum of Δ^6-HOONCA.

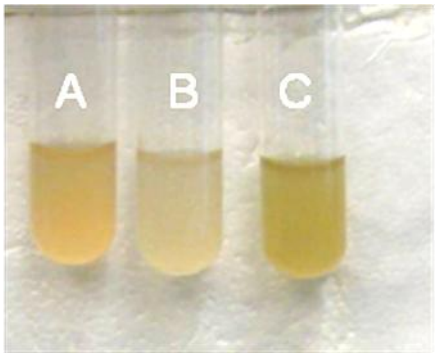


Figure 3.15 Color-comparison of supernatants: A. Δ*cam*B, B. Wild Type, C. Δ*cam*M.

The supernatant of Δ*cam*B also exhibited a noticeable difference in color when compared to wild type (Figure 3.15).

3.3.3 RHA1 and Δ*cam*B Growth on HOONCA Metabolites

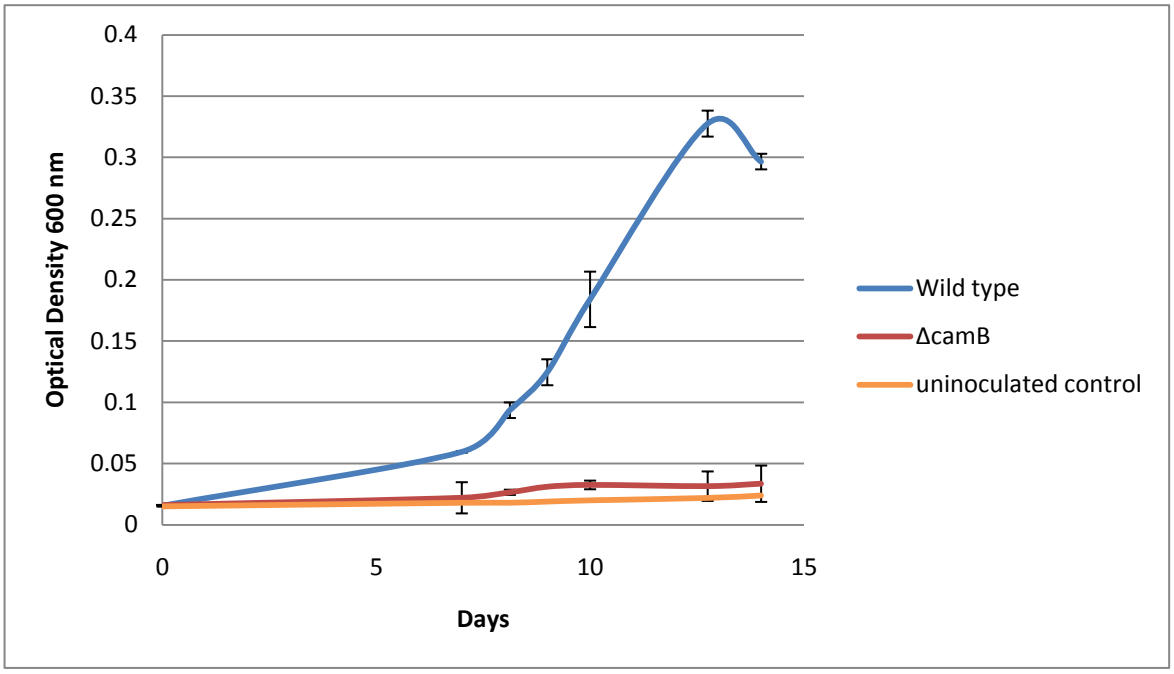


Figure 3.16 Growth of RHA1 and Δ*cam*B on HOONCA metabolites as a carbon and energy source; n=3; error bars indicate standard deviation.

RHA1 and Δ*cam*B were pre-cultured on 2.0 mM cholic acid, then cultured on HOONCA plus Δ^6-HOONCA, harvested from Δ*cam*B supernatant, as the major sources of carbon and energy (Figure 3.16). After seven days, wild type RHA1 entered exponential growth, reaching a maximum OD_{600} of 0.35 ± .02 at around day 13. However Δ*cam*B exhibited no growth on these metabolites, reaffirming that the inactivation of this ABC-transporter inhibits the assimilation and catabolism of these HOONCA compounds.

3.4 Inactivation of the MFS Transporter

CamM was inactivated by in-frame deletion of the *cam*M gene as described in section 2.4 (Figure 3.17).

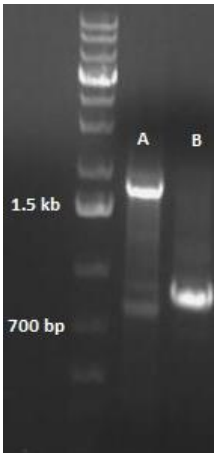


Figure 3.17 Colony PCR electrophoresis gel screening for Δ*cam*M transconjugation: the clone represented in lane A has a wild type copy of *cam*M (1700 base pairs), lane B has a truncated copy (900 base pairs) and was used in subsequent growth experiments.

3.4.1 The Cholic Acid Growth Phenotype of Δ*cam*M

On cholic acid, Δ*cam*M exhibited a specific growth rate of 0.074 h^{-1} with a doubling time of 4.068 hours during exponential growth. The Δ*cam*M mutant appeared to reach the same maximum OD_{600} as wild type RHA1 (Figure 3.18), however this was not a faithful representation of total biomass produced. The Δ*cam*M mutant only reached a final growth yield of 13.6 ± 0.03 μg/ml protein, which is 77.2% the final protein yield of wild type.

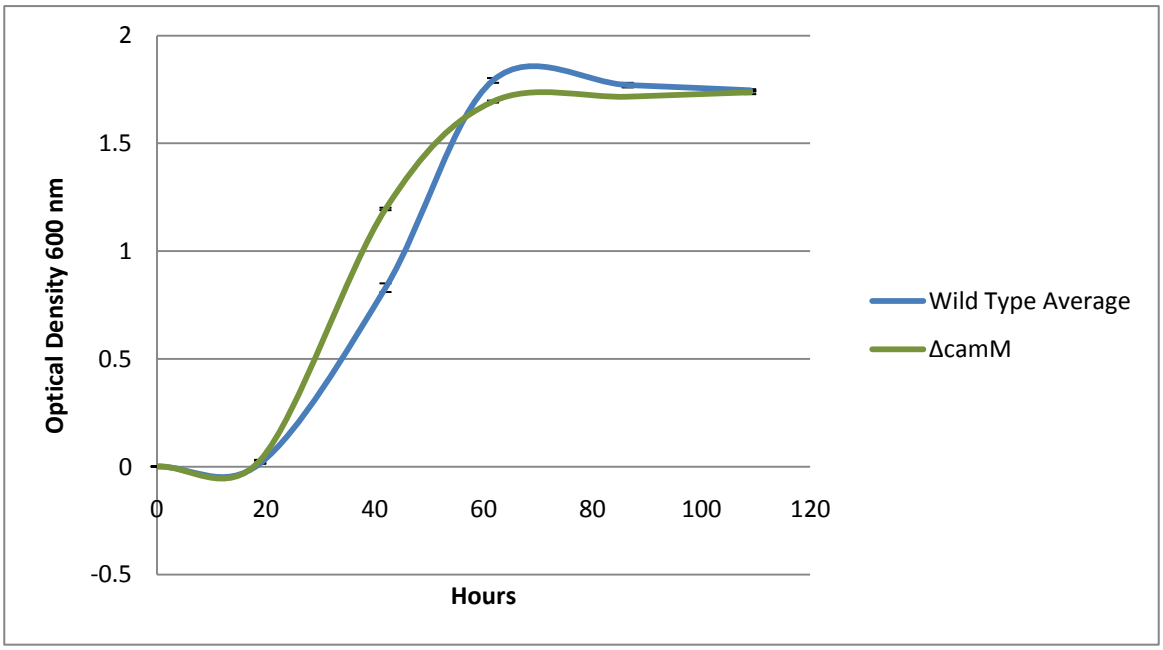


Figure 3.18 Growth of Δ*cam*M on 2.0 mM cholic acid, compared to wild type, measured via OD_{600}; n=3; error bars indicate standard deviation.

The discrepancy between optical density and growth yield is likely due to absorbance at 600 nm of compounds in the supernatant which resulted in the visible dark color (Figure 3.15). The supernatant of Δ*cam*M without cells has an OD_{600} of 0.085, while the cell-free supernatant of RHA1 has an OD_{600} of 0.021. This absorbance may be due to a transformation product of the metabolite or to other material released by Δ*cam*M.

To get an accurate growth curve for Δ*cam*M, a protein assay was performed to calculate the growth yield at selected points in the growth curve and compare it to that of wild type (Figure 3.19). The protein assay confirmed that Δ*cam*M does not exhibit the same growth kinetics as wild type, despite the similar OD_{600} growth curves.

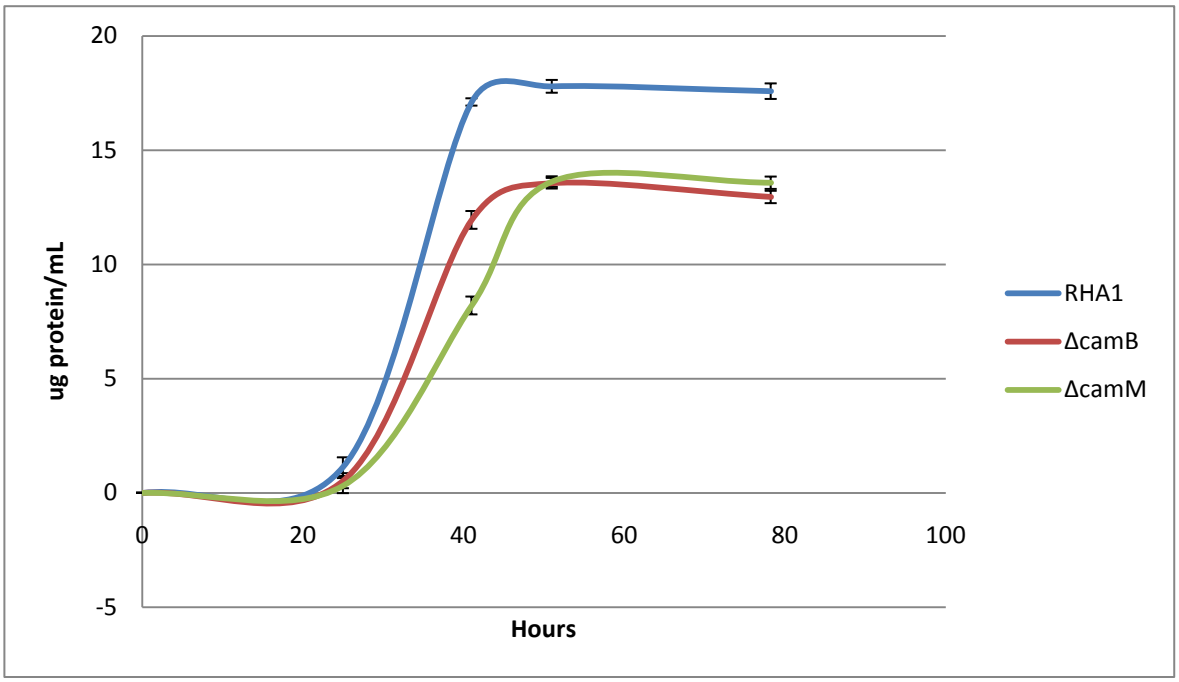


Figure 3.19 Growth of wild type RHA1 and the transporter mutants on 2.0 mM cholic acid, using protein as a measurement of biomass; n=3; error bars indicate standard deviation.

3.4.2 Extracellular Cholic Acid Metabolite Accumulation by Δ*cam*M

The ΔcamM strain accumulated the same metabolites as wild type. However, ΔcamM accumulated THOSBNC (Figure 3.5) to a higher extent than wild type, was unable to reassimilate this compound, and maintained it in the supernatant into late stationary phase (Figure 3.20). This metabolite was identified by its retention time, fragmentation pattern, and molecular ion, as detected by the GCMS, which were consistent over repeated trials (Figure 3.21 and Figure 3.22).

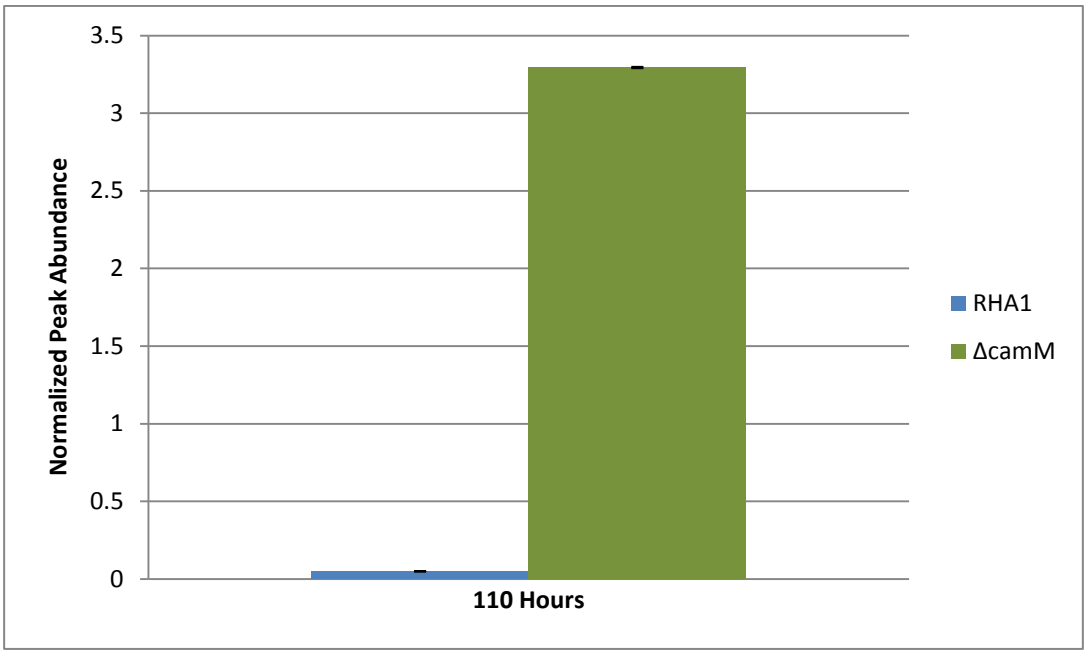


Figure 3.20 THOSBNC accumulation in RHA1 and Δ*cam*M based on normalized GCMS peak abundance; n=3; error bars indicate standard deviation.

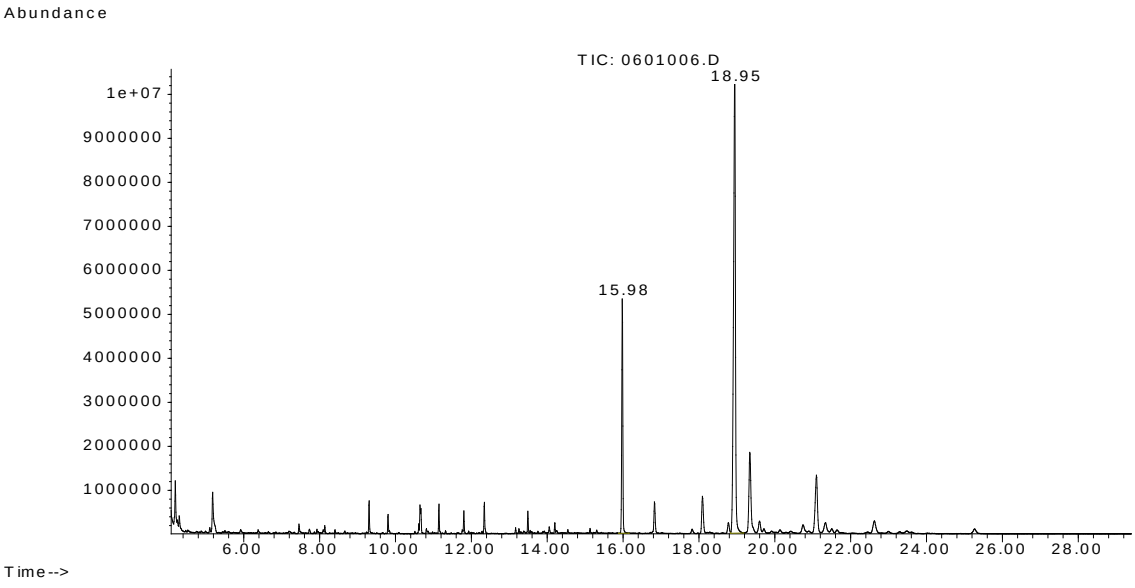


Figure 3.21 Chromatogram of Δ*cam*M stationary phase culture showing peaks of accumulated metabolites. Rt 15.98: cholestane internal standard, rt 18.96: THOSBNC, other peaks are minor metabolites with similar fragmentation patterns as THOSBNC.

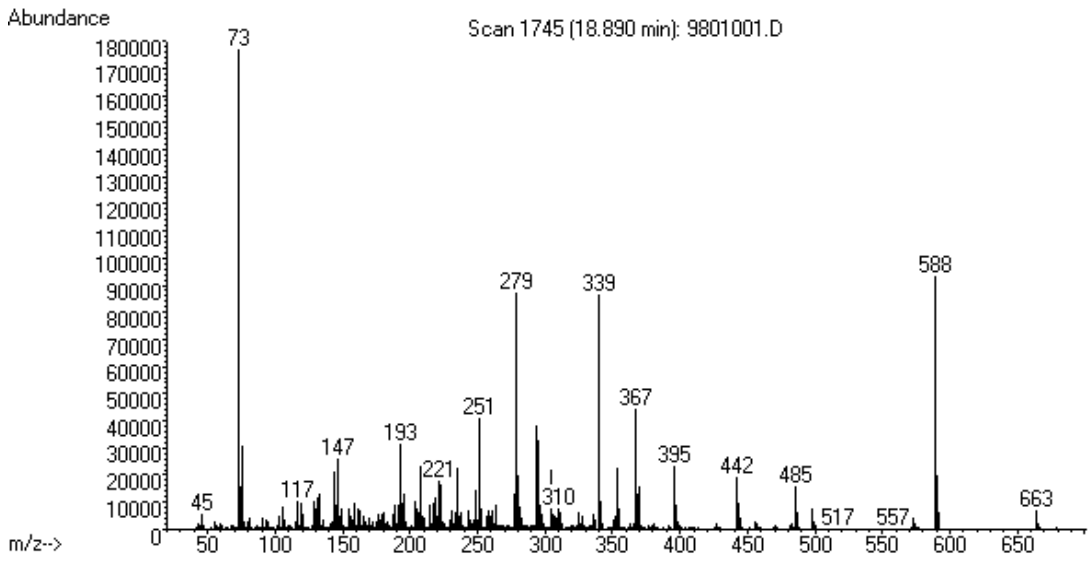


Figure 3.22 Mass spectrum of THOSBNC.

3.4.3 RHA1 and Δ*cam*M Growth on THOSBNC

RHA1 and Δ*cam*M were incubated on THOSBNC, harvested from Δ*cam*M supernatant, as the major source of carbon and energy, as described in section 2.2 (Figure 3.23). Wild-type RHA1 cells entered exponential growth beginning around three days after inoculation, reaching a maximum OD_{600} of 0.09 at around day 8. However Δ*cam*M exhibited no growth on these metabolites, reaffirming that without the inactivated MFS-transporter, Δ*cam*M is unable to reassimilate and catabolize THOSBNC.

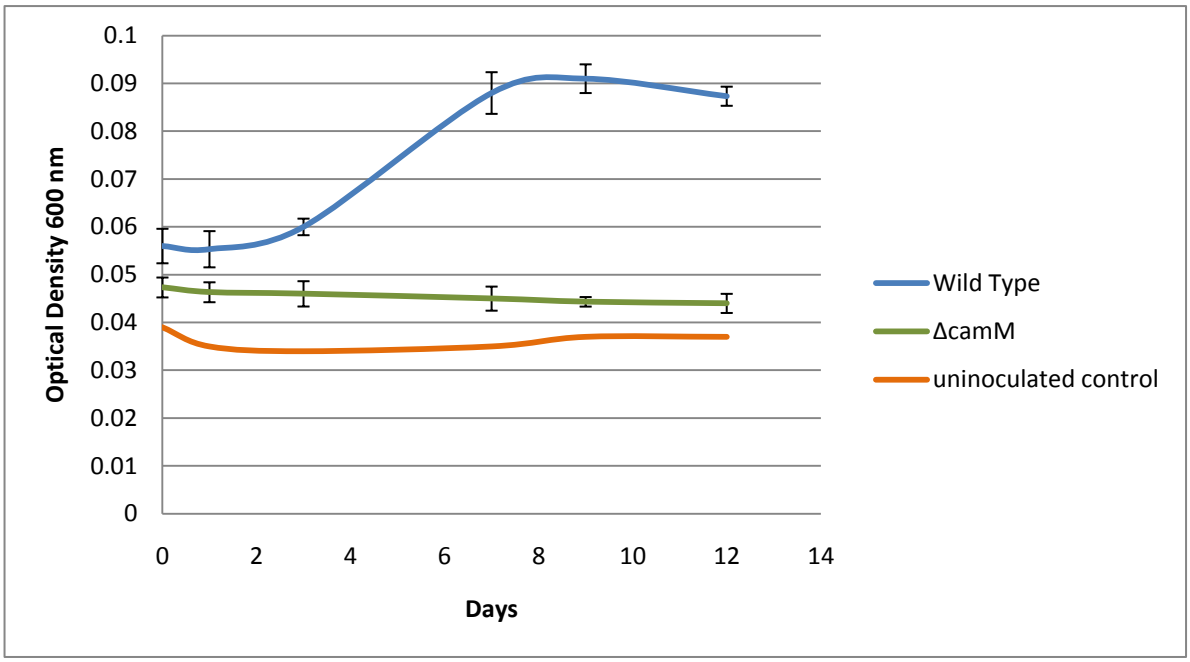


Figure 3.23 Growth of RHA1 and Δ*cam*M on the THOSBNC metabolite as a carbon and energy source; n=3; error bars show standard deviation.

3.5 Cholic Acid Conjugate Growth Phenotype of Δ*cam*M

The Δ*cam*M mutant was grown on the conjugated bile acids glycocholic acid and taurocholic acid (Figure 3.24 A and B respectively) to see if disrupting *cam*M had an effect on the uptake of cholic acid in the conjugated form. On taurocholic acid, Δ*cam*M exhibited the same growth kinetics and final growth yield as observed during growth on cholic acid, and also accumulated THOSBNC without reassimilating the compound. However, growth on glycocholic acid was significantly slower, taking approximately five days instead of two days to reach stationary phase (data not shown). The final growth yield on glycocholic acid was 17.0 μg/ml (±0.3), which is approximately equal to the wild type. Finally, there were no accumulated metabolites in the supernatant of stationary phase Δ*cam*M cultures grown on

glycocholic acid. The Δ*cam*B mutant showed the same growth kinetics and metabolite accumulation in stationary phase from both conjugated bile acids and cholic acid.

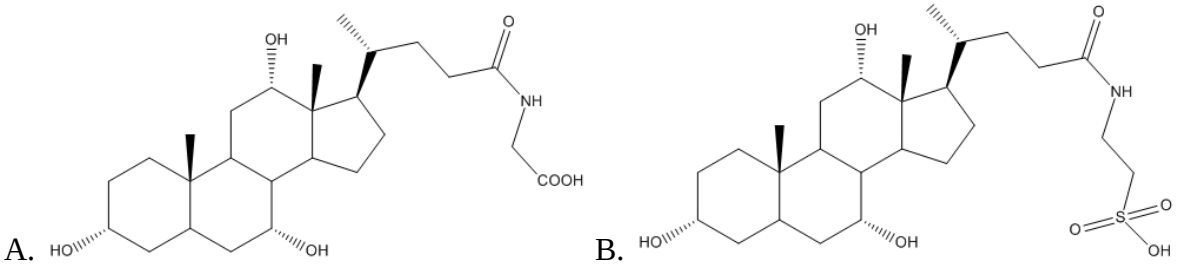


Figure 3.24 Structures of conjugated bile salts: A. glycocholic acid, B. taurocholic acid.

3.6 Complementation

The Δ*cam*B and Δ*cam*M mutants were complemented by insertion of the corresponding genes with their native promoters into the chromosome of the mutant strains. For Δ*cam*B, the full *camABCD* operon was inserted to avoid any issues with protein complex assembly or polar effects on gene expression. Since *cam*M is not part of an operon, only the single gene was inserted for complementation. Insertion complementation was performed in order to avoid any issues with over-expression. Because *cam*M and *cam*ABCD encode membrane proteins, the expression of too many copies may have resulted in unforeseen effects on cellular functioning, which can occur when using a high copy-number expression vector like pTIP.

Both the complementation strains, named Δ*cam*Bc and Δ*cam*Mc, were grown on cholic acid in the same manner as the other strains in this study. Both strains grew slower

than the wild-type on cholic acid. A final protein assay showed Δ*cam*Bc and Δ*cam*Mc reached 98.5% and 89.0%, respectively, of the final growth yield of wild type RHA1 (Figure 3.2). Thus, for both mutants, complementation substantially restored the wild-type cell yield on cholic acid. The somewhat lower yield of each complementation strain may be related to the slower growth rate.

Both strains produced the same metabolites as wild type RHA1 and also, like the wild type, reassimilated these metabolites such that no compounds were detected in the supernatant of stationary phase cultures. Thus, cloning in a wild-type copy of the respective inactivated transporter gene for both Δ*cam*B and Δ*cam*M was sufficient to restore each strains' capacity to uptake all extracellular metabolites. This confirms that CamABCD is required for uptake of the HOONCA metabolites, and CamM is required for uptake of THOSBNC.

Chapter 4: Discussion

4.1 Cholic Acid Uptake and the Potential for Passive Diffusion

Originally, I hypothesized that one of the two upregulated transporters could be required for the uptake of cholic acid across the RHA1 cytoplasmic membrane. In order to be competitive in a natural environment, soil bacteria like RHA1 generally need transporters that give them high affinity for substrates. Specificity for these substrates may vary from narrow (i.e. a single compound) to broad (classes of compounds). The Mce4 system, required for cholesterol but not cholic acid uptake [33], supports the hypothesis of a specific cholic acid uptake system, yet we failed to identify one in this study. As no other transporters were highly upregulated on cholic acid, uptake may occur by a constitutively expressed transporter, perhaps one with broad substrate specificity.

Alternatively, it is possible that cholic acid enters RHA1 via passive diffusion across the cytoplasmic membrane. There is some evidence that cholic acid enters bacteria by this mechanism. The alpha-orientation of all the hydroxyl groups on cholic acid creates distinct hydrophobic and hydrophillic parts of the molecule, which allows it to behave as a detergent [4]. One study found a correlation between hydrophobicity and the rate at which bile salts "flip" across egg phosphatidylcholine vesicles, suggesting that deoxycholic acid would traverse the membrane faster than cholic acid since it is more hydrophobic. This study also concludes that all bile salts would flip through the membrane eventually [62]. However, they also predict that cholesterol would flip faster than any of the bile salts, which seems

inconsistent with the requirement for the Mce4 transporter for growth on cholesterol [33]. Thus it is unclear whether membrane flipping occurs during bile salt catabolism in RHA1.

The only described bacterial bile salt uptake transporter is from the intestinal bacterium *Clostridium scindens*, called BaiG. This protein catalyzes the proton-motive-force-dependent uptake of bile salts [43]. A putative bile salt uptake transporter gene has been found in *Lactococcus johnsonii* [63] but neither this gene nor BaiG have significant similarities to putative transporters in *C. testosteroni* or RHA1 [4]. Thus, it remains unclear whether RHA1 or related organisms employ a transporter for cholic acid uptake, or whether it merely diffuses into the cell.

4.2 A Unifying Scheme for Steroid Degradation

Transient extracellular metabolite accumulation during cholic acid degradation is a general phenomenon seen in diverse microorganisms. I found that RHA1 is no exception. The proposed structures of the RHA1 cholic acid metabolites are similar to those detected in other organisms [4, 24, 45]. What is novel about the RHA1 metabolites is that they retain an isopropionyl group at C17, whereas other metabolites detected in previous studies have a ketone group at this position. This suggests that side-chain degradation may reach completion later in the overall degradation pathway in RHA1 than it does in other cholic acid degrading bacteria.

Despite this distinction, the RHA1 metabolites identified here are consistent with the common pathway of microbial cholic acid degradation [22]. The formation of the seco-steroid THOSBNC suggests that the degradation of rings A and B happens in a similar

fashion in RHA1 as it does in organisms like strains TA441 and Chol1 [24, 45]. In addition, the formation of the HOONCA metabolites also agrees with the seco-steroid pathway constructed from the degradation of other steroid compounds, which all have DOHNAA as the final compound identified before the unknown final steps leading to CO_2 [24]. These metabolites further suggest that the hydroxyl group at C7 is not metabolized until after cleavage of Ring B, and that at C12 is not metabolized until after removal of Ring A.

Results here support the hypothesis that despite different side chain conformations and the attachment of hydroxyl groups at various locations on the steroid nucleus, the degradation of most steroids follows the aforementioned seco-steroid pathway. The main differences appear to lie in the order of side chain degradation relative to A-ring oxidation and B-ring opening, which varies among organisms studied and the steroids degraded.

This study was the first to demonstrate the function of putative cholic acid genes through targeted mutagenesis. Compared to cholesterol and testosterone, the cholic acid pathway is not as well-understood. No catabolic enzymes have yet been purified or characterized. The requirement for transporters involved in cholic acid metabolite uptake has been suggested in previous publications [45], but this study provides the first evidence for and identification of such transporters.

4.3 Support for the Toxic Metabolite Excretion Hypothesis

Like other microorganisms in previous studies, I've demonstrated that RHA1 also transiently accumulates extracellular metabolites during growth on cholic acid. A hypothesis frequently stated is that these metabolites represent precursors to rate-limiting steps in the

cholic acid pathway. At this "bottle neck" in the catabolic pathway, the excess metabolites are excreted into the extracellular environment until the cell is ready to incorporate them back into the cell and further degrade them. This process, including the transporters used in assimilation of the metabolites, would be an adaptive strategy employed by diverse bacteria to maintain low intracellular levels of these metabolites, which are potentially toxic to the cell [45], while maximizing nutritional benefit from cholic acid.

I found additional support for this hypothesis in the growth phenotype on glycocholic acid of Δ*cam*M, which took longer to reach stationary phase than the wild type, yet reached the same final growth yield and did not accumulate THOSBNC. I hypothesize that the initial steps in degradation of glycocholic acid are slower than for cholic acid, due to the altered conformation of the side chain, resulting in a reduced accumulation of THOSBNC, thus eliminating the need for its excretion.

This lack of metabolite accumulation was only observed during growth on glycocholic acid of Δ*cam*M, and not of Δ*cam*B, which showed the same metabolite accumulation in stationary phase from both conjugated bile acids and cholic acid. This could be because Δ*cam*B is required to transport metabolites formed *later* in the pathway, at which point the rate of metabolite generation may be equal for all bile acid substrates.

Finally, efflux transporters for the excretion of these metabolites likely exist. It is possible that these transporters have broad specificity and have a general function in removal of potentially toxic compounds from the bacterial cell. Such transporters would likely be constitutively expressed.

4.4 Two Novel Transporters

Both the ABC and MFS superfamilies are highly diverse; they include transport systems that operate in a range of organisms, from bacteria through humans, to pump a wide variety of substances across biological membranes. Substrate specificity varies greatly, from very specific to very broad, depending on the transporter and the substrate(s) involved [64, 65]. Despite the progress of research on ABC and MFS transporters, many gaps exist in the understanding of their structure and function [64, 66]. Genome sequences have revealed vast numbers of these transporters with unknown functions. There is great need to assign function to transporters in both families in order to advance our general understanding of these important micro-machines.

This study contributes to the general knowledge of both the ABC and MFS superfamilies by identifying novel members of each superfamily with defined transport functions. Further studies on the structures of the CamABCD and CamM systems, as well as investigations on the specificity of each, will contribute to the elucidation of these unique transporters. In particular, since these transporters have novel substrates, they may contribute to understanding the relationship between protein structure and substrate specificity.

4.5 Habitat of Cholic Acid Degraders

This study may provide insight into the environments to which RHA1 has adapted during its evolutionary history. One might assume that RHA1, as well as other free-living microorganisms that can catabolize cholic acid, would have adapted to sequester this

compound from environments in which cholic acid is present in very minute amounts. However, the strategy of metabolite efflux observed here suggests that RHA1 has evolved to deal with cholic acid in much higher concentrations than the limited amount that would likely be present in a given soil sample. Only in environments with a high cholic acid concentration, like the cultures used for this study, would such an efflux process be necessary. This suggests that feces may be a significant habitat for RHA1 and other cholic acid-degrading organisms.

4.6 Implications

Better understanding of steroid metabolite accumulation and uptake may have applications in an industrial context, as this phenomenon may affect the use of whole cell biocatalysis in the manufacture of steroid-related therapeutics. Production of toxic metabolites or metabolite reassimilation could potentially be rate-limiting for a manufacturing process. On the other hand, excretion of desired products could increase the efficiency of a process.

Additionally, there may be environmental implications, as the excretion of metabolites might allow receiving environments to rapidly degrade large quantities of certain steroids discharged by municipal or industrial sewage. The metabolites may have environmental effects and should be studied in this context.

Finally, further studies on the enzymology involved in cholic acid catabolism in RHA1 are required to fully understand the overall catabolic pathway. These accumulated

metabolites could be important and easily available substrates for future activity assays, as they are relatively pure in the supernatant of the Δ*cam*B and Δ*cam*M mutants.

References

1. Hogg JA: **Steroids, the Steroid Community, and Upjohn in Perspective - a Profile of Innovation**. *Steroids* 1992, **57**(12):593-616.

2. Ying GG, Kookana RS, Ru YJ: **Occurrence and fate of hormone steroids in the environment**. *Environ Int* 2002, **28**(6):545-551.

3. Streck G: **Chemical and biological analysis of estrogenic, progestagenic and androgenic steroids in the environment**. *Trac-Trend Anal Chem* 2009, **28**(6):635-652.

4. Philipp B: **Bacterial degradation of bile salts**. *Appl Microbiol Biot* 2011, **89**(4):903-915.

5. Johnston JO: **Aromatase inhibitors**. *Crit Rev Biochem Mol* 1998, **33**(5):375-405.

6. Arthan D, Svasti J, Kittakoop P, Pittayakhachonwut D, Tanticharoen M, Thebtaranonth Y: **Antiviral isoflavonoid sulfate and steroidal glycosides from the fruits of Solanum torvum**. *Phytochemistry* 2002, **59**(4):459-463.

7. Rupprecht R, Holsboer F: **Neuroactive steroids: mechanisms of action and neuropsychopharmacological perspectives**. *Trends Neurosci* 1999, **22**(9):410-416.

8. Lorenzen A, Chapman R, Hendel JG, Topp E: **Persistence and pathways of testosterone dissipation in agricultural soil**. *J Environ Qual* 2005, **34**(3):854-860.

9. Desbrow C, Routledge EJ, Brighty GC, Sumpter JP, Waldock M: **Identification of estrogenic chemicals in STW effluent. 1. Chemical fractionation and in vitro biological screening**. *Environ Sci Technol* 1998, **32**(11):1549-1558.

10. Erb RE, Chew BP, Keller HF: **Relative Concentrations of Estrogen and Progesterone in Milk and Blood, and Excretion of Estrogen in Urine**. *J Anim Sci* 1977, **45**(3):617-626.

11. Belfroid AC, Van der Horst A, Vethaak AD, Schafer AJ, Rijs GBJ, Wegener J, Cofino WP: **Analysis and occurrence of estrogenic hormones and their glucuronides in surface water and waste water in The Netherlands**. *Sci Total Environ* 1999, **225**(1-2):101-108.

12. Jobling S, Nolan M, Tyler CR, Brighty G, Sumpter JP: **Widespread sexual disruption in wild fish**. *Environ Sci Technol* 1998, **32**(17):2498-2506.

13. Shore LS, Kapulnik Y, Gurevich M, Wininger S, Badamy H, Shemesh M: **Induction of phytoestrogen production in Medicago sativa leaves by irrigation with sewage water**. *Environ Exp Bot* 1995, **35**(3):363-369.

14. Thomas KV, Hurst MR, Matthiessen P, McHugh M, Smith A, Waldock MJ: **An assessment of in vitro androgenic activity and the identification of environmental androgens in United Kingdom estuaries**. *Environ Toxicol Chem* 2002, **21**(7):1456-1461.

15. Fernandes P, Cruz A, Angelova B, Pinheiro HM, Cabral JMS: **Microbial conversion of steroid compounds: recent developments**. *Enzyme Microb Tech* 2003, **32**(6):688-705.

16. Donova MV: **Transformation of steroids by actinobacteria: A review**. *Appl Biochem Micro+* 2007, **43**(1):1-14.

17. Malaviya A, Gomes J: **Androstenedione production by biotransformation of phytosterols**. *Bioresour Technol* 2008, **99**(15):6725-6737.

18. Donova MV, Dovbnya DV, Sukhodolskaya GV, Khomutov SM, Nikolayeva VM, Kwon I, Han K: **Microbial conversion of sterol-containing soybean oil production waste**. *J Chem Technol Biot* 2005, **80**(1):55-60.

19. Dias ACP, Fernandes P, Cabral JMS, Pinheiro HM: **Isolation of a biodegradable sterol-rich fraction from industrial wastes**. *Bioresource Technol* 2002, **82**(3):253-260.

20. Moldowan JM, Dahl J, Mccaffrey MA, Smith WJ, Fetzer JC: **Application of Biological Marker Technology to Bioremediation of Refinery by-Products**. *Energ Fuel* 1995, **9**(1):155-162.

21. Jacobsen AM, Lorenzen A, Chapman R, Topp E: **Persistence of testosterone and 17 beta-estradiol in soils receiving swine manure or municipal biosolids**. *J Environ Qual* 2005, **34**(3):861-871.

22. Hayakawa S: **Microbial Transformation of Bile-Acids - a Unified Scheme for Bile-Acid Degradation, and Hydroxylation of Bile-Acids**. *Z Allg Mikrobiol* 1982, **22**(5):309-326.

23. Van der Geize R, Yam K, Heuser T, Wilbrink MH, Hara H, Anderton MC, Sim E, Dijkhuizen L, Davies JE, Mohn WW *et al*: **A gene cluster encoding cholesterol catabolism in a soil actinomycete provides insight into Mycobacterium tuberculosis survival in macrophages**. *P Natl Acad Sci USA* 2007, **104**(6):1947-1952.

24. Horinouchi M, Kurita T, Hayashi T, Kudo T: **Steroid degradation genes in Comamonas testosteroni TA441: Isolation of genes encoding a Delta 4(5)-isomerase and 3 alpha- and 3 beta-dehydrogenases and evidence for a 100 kb steroid degradation gene hot spot**. *J Steroid Biochem* 2010, **122**(4):253-263.

25. Horinouchi M, Hayashi T, Kudo T: **The genes encoding the hydroxylase of 3-hydroxy-9,10-secoandrosta-1,3,5(10)-triene-9,17-dione in steroid degradation in Comamonas testosteroni TA441**. *J Steroid Biochem* 2004, **92**(3):143-154.

26. Mobus E, Maser E: **Molecular cloning overexpression, and characterization of steroid-inducible 3 alpha-hydroxysteroid dehydrogenase/carbonyl reductase from Comamonas testosteroni - A novel member of the short-chain dehydrogenase/reductase superfamily**. *J Biol Chem* 1998, **273**(47):30888-30896.

27. Horinouchi M, Hayashi T, Yamamoto T, Kudo T: **A new bacterial steroid degradation gene cluster in Comamonas testosteroni TA441 which consists of aromatic-compound degradation genes for seco-steroids and 3-ketosteroid dehydrogenase genes**. *Appl Environ Microb* 2003, **69**(8):4421-4430.

28. Horinouchi M, Hayashi T, Koshino H, Kudo T: **ORF18-disrupted mutant of Comamonas testosteroni TA441 accumulates significant amounts of 9,17-dioxo-1,2,3,4,10,19-hexanorandrostan-5-oic acid and its derivatives after incubation with steroids**. *J Steroid Biochem* 2006, **101**(1):78-84.

29. Ma YF, Zhang Y, Zhang JY, Chen DW, Zhu YQ, Zheng HJ, Wang SY, Jiang CY, Zhao GP, Liu SJ: **The Complete Genome of Comamonas testosteroni Reveals Its Genetic Adaptations to Changing Environments**. *Appl Environ Microb* 2009, **75**(21):6812-6819.

30. Hu YM, van der Geize R, Besra GS, Gurcha SS, Liu A, Rohde M, Singh M, Coates A: **3-Ketosteroid 9 alpha-hydroxylase is an essential factor in the pathogenesis of Mycobacterium tuberculosis**. *Mol Microbiol* 2010, **75**(1):107-121.

31. Cole ST, Brosch R, Parkhill J, Garnier T, Churcher C, Harris D, Gordon SV, Eiglmeier K, Gas S, Barry CE *et al*: **Deciphering the biology of Mycobacterium tuberculosis from the complete genome sequence**. *Nature* 1998, **393**(6685):537-+.

32. Senaratne RH, Sidders B, Sequeira P, Saunders G, Dunphy K, Marjanovic C, Reader JR, Lima P, Chan S, Kendall S *et al*: **Mycobacterium tuberculosis strains disrupted in mce3 and mce4 operons are attenuated in mice**. *J Med Microbiol* 2008, **57**(2):164-170.

33. Mohn WW, van der Geize R, Stewart GR, Okamoto S, Liu J, Dijkhuizen L, Eltis LD: **The Actinobacterial mce4 Locus Encodes a Steroid Transporter**. *J Biol Chem* 2008, **283**(51):35368-35374.

34. van der Geize R, Dijkhuizen L: **Harnessing the catabolic diversity of rhodococci for environmental and biotechnological applications**. *Curr Opin Microbiol* 2004, **7**(3):255-261.

35. Rosloniec KZ, Wilbrink MH, Capyk JK, Mohn WW, Ostendorf M, van der Geize R, Dijkhuizen L, Eltis LD: **Cytochrome P450 125 (CYP125) catalyses C26-hydroxylation to initiate sterol side-chain degradation in Rhodococcus jostii RHA1**. *Mol Microbiol* 2009, **74**(5):1031-1043.

36. Eltis LD, Capyk JK, Kalscheuer R, Stewart GR, Liu J, Kwon H, Zhao R, Okamoto S, Jacobs WR, Mohn WW: **Mycobacterial Cytochrome P450 125 (Cyp125) Catalyzes the Terminal Hydroxylation of C27 Steroids**. *J Biol Chem* 2009, **284**(51):35534-35542.

37. Yam KC, Okamoto S, Roberts JN, Eltis LD: **Adventures in Rhodococcus - from steroids to explosives**. *Can J Microbiol* 2011, **57**(3):155-168.

38. van der Geize R, Hessels GI, van Gerwen R, van der Meijden P, Dijkhuizen L: **Unmarked gene deletion mutagenesis of kstD, encoding 3-ketosteroid Delta1-dehydrogenase, in Rhodococcus erythropolis SQ1 using sacB as counter-selectable marker**. *FEMS Microbiol Lett* 2001, **205**(2):197-202.

39. van der Geize R, Hessels GI, van Gerwen R, van der Meijden R, Dijkhuizen L: **Molecular and functional characterization of kshA and kshB, encoding two components of 3-ketosteroid 9 alpha-hydroxylase, a class IA monooxygenase, in Rhodococcus erythropolis strain SQ1**. *Mol Microbiol* 2002, **45**(4):1007-1018.

40. Horinouchi M, Hayashi T, Koshino H, Yamamoto T, Kudo T: **Gene encoding the hydrolase for the product of the meta-cleavage reaction in testosterone degradation by Comamonas testosteroni**. *Appl Environ Microb* 2003, **69**(4):2139-2152.

41. Hofmann AF, Mysels KJ: **Bile-Salts as Biological Surfactants**. *Colloid Surface* 1988, **30**(1-2):145-173.

42. Helenius A, Simons K: **Solubilization of Membranes by Detergents**. *Biochim Biophys Acta* 1975, **415**(1):29-79.

43. Ridlon JM, Kang DJ, Hylemon PB: **Bile salt biotransformations by human intestinal bacteria**. *J Lipid Res* 2006, **47**(2):241-259.

44. Bernstein H, Bernstein C, Payne CM, Dvorak K: **Bile acids as endogenous etiologic agents in gastrointestinal cancer**. *World J Gastroentero* 2009, **15**(27):3329-3340.

45. Birkenmaier A, Holert J, Erdbrink H, Moeller HM, Friemel A, Schoenenberger R, Suter MJF, Klebensberger J, Philipp B: **Biochemical and genetic investigation of**

initial reactions in aerobic degradation of the bile acid cholate in Pseudomonas sp strain Chol1. *J Bacteriol* 2007, **189**(20):7165-7173.

46. Bortolini O, Medici A, Poli S: **Biotransformations on steroid nucleus of bile acids**. *Steroids* 1997, **62**(8-9):564-577.

47. Goodfellow M, Williams ST: **Ecology of Actinomycetes**. *Annu Rev Microbiol* 1983, **37**:189-216.

48. McLeod MP, Warren RL, Hsiao WWL, Araki N, Myhre M, Fernandes C, Miyazawa D, Wong W, Lillquist AL, Wang D *et al*: **The complete genome of Rhodococcus sp RHA1 provides insights into a catabolic powerhouse**. *P Natl Acad Sci USA* 2006, **103**(42):15582-15587.

49. Finnerty WR: **The Biology and Genetics of the Genus Rhodococcus**. *Annu Rev Microbiol* 1992, **46**:193-218.

50. Bell KS, Philp JC, Aw DWJ, Christofi N: **A review - The genus Rhodococcus**. *Journal of Applied Microbiology* 1998, **85**(2):195-210.

51. Martinkova L, Uhnakova B, Patek M, Nesvera J, Kren V: **Biodegradation potential of the genus Rhodococcus**. *Environ Int* 2009, **35**(1):162-177.

52. Elder RT: **Molecular-Cloning - a Laboratory Manual - Maniatis,T, Pritsch,Er, Sambrook,J**. *Bioscience* 1983, **33**(11):721-722.

53. Bauchop T, Elsden SR: **The growth of micro-organisms in relation to their energy supply**. *J Gen Microbiol* 1960, **23**:457-469.

54. Schafer A, Tauch A, Jager W, Kalinowski J, Thierbach G, Puhler A: **Small Mobilizable Multipurpose Cloning Vectors Derived from the Escherichia-Coli Plasmids Pk18 and Pk19 - Selection of Defined Deletions in the Chromosome of Corynebacterium-Glutamicum**. *Gene* 1994, **145**(1):69-73.

55. Bierman M, Logan R, Obrien K, Seno ET, Rao RN, Schoner BE: **Plasmid Cloning Vectors for the Conjugal Transfer of DNA from Escherichia-Coli to Streptomyces Spp**. *Gene* 1992, **116**(1):43-49.

56. Nakashima N, Tamura T: **Isolation and characterization of a rolling-circle-type plasmid form Rhodococcus erythropolis and application of the plasmid to multiple-recombinant-protein expression**. *Appl Environ Microb* 2004, **70**(9):5557-5568.

57. Kalscheuer R, Arenskotter M, Steinbuchel A: **Establishment of a gene transfer system for Rhodococcus opacus PD630 based on electroporation and its**

application for recombinant biosynthesis of poly(3-hydroxyalkanoic acids). *Appl Microbiol Biot* 1999, **52**(4):508-515.

58. Goncalves ER, Hara H, Miyazawa D, Davies JE, Eltis LD, Mohn WW: **Transcriptomic assessment of isozymes in the biphenyl pathway of Rhodococcus sp. strain RHA1**. *Appl Environ Microbiol* 2006, **72**(9):6183-6193.

59. LeBlanc JC, Goncalves ER, Mohn WW: **Global response to desiccation stress in the soil actinomycete Rhodococcus jostii RHA1**. *Appl Environ Microbiol* 2008, **74**(9):2627-2636.

60. Mathieu JM, Mohn WW, Eltis LD, LeBlanc JC, Stewart GR, Dresen C, Okamoto K, Alvarez PJ: **7-ketocholesterol catabolism by Rhodococcus jostii RHA1**. *Appl Environ Microbiol* 2010, **76**(1):352-355.

61. Hara H, Stewart GR, Mohn WW: **Involvement of a novel ABC transporter and monoalkyl phthalate ester hydrolase in phthalate ester catabolism by Rhodococcus jostii RHA1**. *Appl Environ Microbiol* 2010, **76**(5):1516-1523.

62. Cabral DJ, Small DM, Lilly HS, Hamilton JA: **Transbilayer Movement of Bile-Acids in Model Membranes**. *Biochemistry-Us* 1987, **26**(7):1801-1804.

63. Elkins CA, Savage DC: **Identification of genes encoding conjugated bile salt hydrolase and transport in Lactobacillus johnsonii 100-100**. *J Bacteriol* 1998, **180**(17):4344-4349.

64. Paulsen IT: **Multidrug efflux pumps and resistance: regulation and evolution**. *Curr Opin Microbiol* 2003, **6**(5):446-451.

65. Maloney PC, Davidson AL: **ABC transporters: how small machines do a big job**. *Trends Microbiol* 2007, **15**(10):448-455.

66. Schneider E, Hunke S: **ATP-binding-cassette (ABC) transport systems: Functional and structural aspects of the ATP-hydrolyzing subunits/domains**. *Fems Microbiol Rev* 1998, **22**(1):1-20.